

6233

402695

402 695

ASD-TDR-63-244

A NUCLEAR-PHOTON ENERGY
CONVERSION STUDY

TECHNICAL DOCUMENTARY REPORT NO. ASD-TDR-63-244

March 1963

Flight Accessories Laboratory
Aeronautical Systems Division
Air Force Systems Command
Wright-Patterson Air Force Base, Ohio

Project No. 8173, Task No. 817301-17

(Prepared under Contract No. AF 33(657)-8527
by Armour Research Foundation of Illinois Institute of Technology,
Technology Center, Chicago 16, Illinois
Authors: H. V. Watts, M. D. Oestreich, R. J. Robinson)

ASTIA
REF ID: A62112
MAY 1 1963
TISIA

NOTICES

When Government drawings, specifications, or other data are used for any purpose other than in connection with a definitely related Government procurement operation, the United States Government thereby incurs no responsibility nor any obligation whatsoever; and the fact that the Government may have formulated, furnished, or in any way supplied the said drawings, specifications, or other data, is not to be regarded by implication or otherwise as in any manner licensing the holder or any other person or corporation, or conveying any rights or permission to manufacture, use, or sell any patented invention that may in any way be related thereto.

Qualified requesters may obtain copies of this report from the Armed Services Technical Information Agency, (ASTIA), Arlington Hall Station, Arlington 12, Virginia.

This report has been released to the Office of Technical Services, U.S. Department of Commerce, Washington 25, D. C., in stock quantities for sale to the general public.

Copies of this report should not be returned to the Aeronautical Systems Division unless return is required by security considerations, contractual obligations, or notice on a specific document.

FOREWORD

This report was prepared by Armour Research Foundation of Illinois Institute of Technology as a final report covering the research on Contract AF 33(657)-8527, Project No. 8173, "Static Energy Conversion", Task No. 817301, "Photoelectric Power", Subtask-17. The work was administered under the direction of Flight Accessories Laboratory, Aeronautical Systems Division. Mr. F. M. Plauché represented ASD on this contract.

The research described herein began in April 1962, and continued through February 1963. Although the research was a group effort, the chief contributors were: H. V. Watts, R. J. Robinson, and M. D. Oestreich. This technical report is unclassified.

ABSTRACT

A double energy conversion technique was studied for aerospace use as a radioisotope powered 10 watt electrical output power source. In this technique, beta particles from a radioisotope are absorbed by a luminescent material which emits a multiplicity of low energy photons. These photons are then converted to electrical energy by a photovoltaic device. The three components (radioisotope, phosphor, and photovoltaic cell) are discussed individually and then in combination in various geometries of source-phosphor and phosphor-photovoltaic converter. Nuclear radiation effects on the phosphor and photovoltaic materials restrict the choice of the radioisotope to a low energy beta emitter; and temperature effects limit the number of "unit power cells" which may be stacked in one bundle. These effects are more pronounced in silicon photovoltaic converters than in ZnCdS: Cu type phosphors. A ten watt output power source fabricated with currently available materials (Pm-147, ZnCdS: Cu, and silicon photovoltaic cells) would have an overall energy conversion efficiency of about 0.2 percent and a power per weight ratio of 4 mw/lb. It is estimated that the power per weight could be increased by a factor of ten to forty if certain "ideal" materials were available. The rapid decrease in photovoltage and energy conversion efficiency of silicon cells at low illumination intensities causes an appreciable loss in the overall efficiency of such power source.

PUBLICATION REVIEW

The publication of this report does not constitute approval by the Air Force of the findings or conclusions herein. It is published for the exchange and stimulation of ideas.

TABLE OF CONTENTS

INTRODUCTION AND SUMMARY	1
MATERIALS	3
Radioisotope Beta Sources	3
Photovoltaic Converters	5
Phosphors	8
NUCLEAR RADIATION EFFECTS	13
TEMPERATURE EFFECTS	16
Temperature Effect on Efficiency	16
Temperature Restriction on Power Source Geometry	18
SOURCE-PHOSPHOR GEOMETRY	20
Back Surface Beta Excitation	20
Matrix Distribution of Source in Large Crystal	
Phosphor	28
Source-Phosphor Powder Mix	30
Power per Unit Weight Considerations	34
PHOSPHOR-PHOTOVOLTAIC CONVERTER GEOMETRY	39
Single Crystal Phosphor-Photovoltaic Converter	39
DESIGN OF TEN WATT POWER SOURCE	42
Prototype Unit Power Cell	42
Ten Watt Source Design	43
Future Improvements on Power Source	44
CONCLUSIONS	46
LIST OF REFERENCES	47
APPENDIX I - DETERMINATION OF THE TEMPERATURE OF STACKED POWER UNITS	49
APPENDIX II - CONCEPTUAL DESIGN OF TEN WATT POWER SOURCE BASED ON CURRENTLY AVAILABLE MATERIALS	54
APPENDIX III - PHOTOVOLTAIC EFFICIENCY AND LARGE BAND GAP SEMICONDUCTORS	57

LIST OF FIGURES

Figure No.		Page
1	Spectral Response of Silicon p-n Photovoltaic Cells	6
2	Effect of Illumination Intensity on the Energy Conversion Efficiency and Open Circuit Voltage of a Silicon p-n Photovoltaic Cell	7
3	Effect of Cobalt-60 Gamma Radiation on the Relative Efficiencies of a ZnCdS:Cu Phosphor and a Silicon p-n Photovoltaic Cell	14
4	Effect of Temperature on the Relative Efficiencies of a ZnCdS:Cu Phosphor and a Silicon p-n Photovoltaic Cell	17
5	Effect of Temperature on the Relative Efficiencies of ZnS:Cu and ZnS:Ag Phosphors	19
6	Phosphor Container	23
7	Strontium-90 Beta Source Holder and Sample Drawer	24
8	Effect of Phosphor Thickness on Light Output with Back-Surface Strontium-90 Beta Excitation	26
9	Geometry of Beta Source and Single Crystal Phosphor	29
10	Apparatus for Containment and Evaluation of Phosphor-Source Mixtures	32
11	Dependence of Source-Phosphor Efficiency, Silicon Cell Efficiency, and Total Efficiency on Amount of Promethium-147 per Unit Area	35
12	Effect of Phosphor-Source Ratio (mg/curie) on Total Efficiency	36
13	Dependence of Power per Unit Weight on Amount of Promethium-147 per Unit Area	38
14	One-Dimensional, Steady Heat Flow Model	49
15	Individual Cell	50
16	Conceptual Design of Ten Watt Power Source	55

LIST OF TABLES

Table		Page
1	Characteristics of Beta Emitting Radioisotopes	4
2	Emission Peak and Energy Yield of Several Zinc Sulfide Type Phosphors Excited by Nuclear Radiation	10
3	Relative Light Output, L, per Unit Area of Various Phosphors Under Ultraviolet Excitation as Detected by a Silicon Photovoltaic Cell	11
4	Calculated Relative Light Output for Back Surface Sr^{90} Excited Phosphors of Various Transparency	22
5	Efficiency Data of Phosphor-Source Mix at Various Loading Ratios and Thicknesses	33

INTRODUCTION AND SUMMARY

The overall objective of this research project is to design a nuclear radiation powered electrical energy source based on the following energy conversion scheme:

1. A primary source of nuclear radiation from a radioisotope;
2. A material which absorbs the nuclear particles and re-emits a multiplicity of low energy photons (visible), i. e., a luminescent material;
3. A converter of low energy photons to electrical energy, i. e., a photovoltaic device.

The device is to have a ten watt output at 28 volts or less.

Power sources of this type have been fabricated and have been described in literature and patents (Ref. 1, 2, 3). The devices which have been fabricated to date have been of very low power output (tens of microwatts) and were reported to have overall energy conversion efficiencies of the order of 0.1 to 1.0 percent. In general, these devices have utilized a promethium-147 beta source exciting a powdered zinc sulfide or zinc sulfide-cadmium sulfide phosphor with a silicon photovoltaic cell as the final converter.

The first two steps of this energy conversion scheme constitute the essence of a nuclear light source. Considerable effort has been expended on the development of beta-ray excited light sources (Ref. 4-10). These sources are usually designed to have visible photon outputs which peak near the maximum response of the eye, i. e., at a wavelength of about 520 millimicrons, and the "high brightness" sources have light outputs of the order of 5000 microlamberts or about 8 microwatts/cm². Using data from the references on commercially available nuclear light sources (Ref. 11), the overall energy efficiency of the light sources is one to two percent. The energy conversion efficiency of the phosphors used is 20 to 25 percent, and thus there is a combined loss in the beta particle utilization and the optical absorption and reflection that reduces the overall efficiency by a factor of ten to fifty.

Early in this project we chose one or two candidate materials for each of the three components (the photovoltaic converter, the luminescent material, and the radioisotope) of the energy conversion scheme. These choices were based on a literature and information search on materials which exist today as essentially "off-the-shelf" items; and these choices

Manuscript released by authors February 1963 for publication as an ASD Technical Documentary Report.

are, if not the best, at least representative of the necessary components. The photovoltaic converter choice was the p-n or n-p junction silicon photovoltaic cell; a transparent single crystal of silver or copper doped cadmium sulfide was the luminescent material choice; and the high specific activity radioisotopes of promethium-147 and strontium-90 were considered.

Delays in obtaining luminescent single crystal cadmium sulfide materials have limited the amount of experimental work which could be performed on these single crystal phosphors. Even though the single crystal phosphor is believed to be a better choice than powdered phosphors, appreciable work was done with the powdered zinc sulfide, cadmium sulfide type phosphors. A great deal of the information obtained with the powdered phosphors may be applied to the large single crystal material.

The candidate materials have been studied for their use in a ten watt output device where the ambient conditions of temperature and nuclear radiation become appreciably more severe than for the tenths of milliwatt output devices mentioned previously. Three different geometries of the radioisotope source and phosphor have been considered. One geometry is the use of a thin disc type source, which is placed directly on the surface of the phosphor, providing a back surface beta excitation to the phosphor. The second geometry is an intimate powder mix of source and phosphor, and the third geometry is the loading of a single crystal phosphor with the radioisotope placed in a matrix pattern in the phosphor crystal. The phosphor-photovoltaic converter optical coupling is considered for the case of using silicon photovoltaic cells. Also, a single crystal phosphor-photovoltaic converter combination in CdS is considered. This combination device would have the best possible optical coupling.

Calculations were performed to find the operational temperature reached in a double conversion power source of this type for a power device of the mixed source-phosphor type. The number of individual power cells which may be stacked is limited by the temperature. A conceptual design of a ten watt output device is then discussed on the basis of the above described work.

A major point which is obvious throughout this study is the fact that the illumination intensities on the photovoltaic converter will be very low compared to the intensities of concern for solar photovoltaic cells. This fact suggests the consideration of photovoltaic materials with wider junction transition regions where it is expected that there may be less efficiency at high light levels, but a less rapid decrease in efficiency at low light levels.

MATERIALS

Radioisotope Beta Sources

The radioisotope sources considered are the long lived radioisotopes (half-lives of years) which are essentially pure beta particle emitters. Several beta emitting radioisotopes are listed in Table 1 with their characteristic half-lives and maximum beta particle energy. The ideal or theoretical maximum specific activity has been calculated for each radioisotope and the specific activity available today is also listed. Promethium-147 and tritium are available at essentially their ideal specific activities, and strontium-90 is available at about one-half of its ideal specific activity. The specific power for each radioisotope is calculated using the average beta energy per disintegration, which is about one-third of the maximum beta energy (Ref. 12). Specific power per gram is then calculated based upon the currently available specific activity.

The ideal specific power per gram does not differ greatly for the various radioisotopes, and the specific powers per gram available today from strontium-90, promethium-147, and tritium are practically identical. A major difference between these three materials is in the range of their beta particles. The range listed in Table 1 is for the maximum energy beta of the radioisotope's beta energy emission distribution. Actually, about 80 to 90 percent of the total beta energy emitted from a radioisotope is absorbed within one-half of the maximum beta range (Ref. 12).

In this program we considered the use of strontium-90 and promethium-147. The high energy beta (2.2 Mev) from yttrium-90, the daughter product of strontium-90, provides a long range and thus reduces the self absorption losses in certain source configurations. On the other hand, this high energy beta creates a larger source of potential radiation damage due both to its direct effect on the phosphor and to the bremsstrahlung radiation which it produces.

The total intensity (number of photons times the photon energy) of bremsstrahlung from monoenergetic beta rays in thick targets is given by:

$$I = kZE^2$$

where

I = bremsstrahlung intensity

k = constant

Z = atomic number of beta absorber

E = beta energy (Mev).

Published values for the constant k vary widely in the range of 10^{-4} to 10^{-3} (Ref. 13). The spectral distribution of bremsstrahlung photons is a straight line function with the maximum photon energy equal to the beta ray energy.

Table 1
CHARACTERISTICS OF BETA EMITTING RADIOISOTOPES

Radioisotope and Compounds	Half Life $T_{1/2}$ (yrs.)	Maximum Energy of β (Mev)	Range of Maximum Energy β (mg/cm 2)	Theoretical Maximum Specific Activity (curies/cm)		Currently Available Specific Activity (a) (curies/gm)		Specific Power Per Curie (μ w/curie) Per Gram (mw/gm)	
				Activity (a) (curies/cm)	Activity (a) (curies/gm)	Per Curie (μ w/curie)	Per Gram (mw/gm)		
Promethium-147 Pm_2O_3	2.6	0.22	57	945	860	380	330	280	
Strontium-90 (Y-90) SrTiO_3	28	0.61 - 2.2	1100	142	68	5460	370	130	
SrCl_2				69	33			210	
Thallium-204 TlNO_3	4	0.77	280	438	3.0	1470	4.4	3.4	
Krypton-85 (gas)	10.3	0.69	240	410	336 2.3	1360	28		
Tritium-(H-3) (gas)	12.4	0.018	0.72	9730	21 (0.08 c/cc) 9700 (2.59 c/cc)	33	320	-	

(a) Data from ORNL Isotopes Catalog and private communication with R. S. Pressly of ORNL.

(b) Based on currently available specific activity.

The number of photons at the maximum energy is zero, and the number of photons at zero energy is thus $2kZE$.

Strontium-90 will therefore produce a bremsstrahlung intensity of 100 times that from promethium-147, for equivalent curie amounts and the same absorber; and the photon energy from strontium-90 bremsstrahlung would be about ten times that for promethium. Martin Marietta Corporation (Ref. 14) has made calculations on the bremsstrahlung from kilocurie SrTiO_3 sources. They found an average bremsstrahlung photon energy of 236 Kev and a surface bremsstrahlung dose rate of about 10^5 R/hr from a 12,000 curie source cylinder 1.48 inches in diameter and 4.55 inches high. The effective Z for SrTiO_3 is 26 while the effective Z for phosphors is from 27 to 44. ($\text{ZnS} - Z = 27$; $\text{CdS} - Z = 44$). Martin's calculations were checked against measurements made on a 1000 curie source. The average bremsstrahlung photon energy from promethium-147 betas absorbed in zinc sulfide is about 20 kev (Ref. 7).

Photovoltaic Converters

The conversion of radiant energy to electrical energy in a photovoltaic cell arises by inducing a photogenerated non-equilibrium distribution of charge carriers in the immediate neighborhood of a potential assymmetry or barrier. The non-equilibrium distribution of charge gives rise to a voltage change in the barrier and to a net current; the amount of change in the equilibrium barrier potential is the induced photovoltage. Commercially available photovoltaic cells include selenium cells, copper oxide cells, p-n junction silicon cells, n-p junction silicon cells, and recently gallium arsenide junction cells. In the research and development stage are CdS barrier layer cells, and CdTe junction cells. Probably other materials of which we have no direct knowledge are in the research stage of photovoltaic cell development. The high energy conversion efficiency, the advanced state of the art, and the commercial availability of the silicon photovoltaic cell have made this material the tentative choice for the photovoltaic converter in this power source study.

The conversion efficiency of photovoltaic cells has been discussed in detail in terms of certain loss mechanisms (Ref. 15). Energy conversion efficiencies of ten to fourteen percent in silicon p-n junction solar cells are reported for the sunlight spectrum and sunlight intensities. The response versus the wavelength of incident light for such cells is shown in Figure 1 (Ref. 16). An appreciable amount of the energy of sunlight is not within the spectral response region of silicon, and thus one would expect energy conversion efficiencies of about twenty percent or more for light which is in the wavelength region between 0.5 to 1.0 microns.

These high energy conversion efficiencies are realized, however, only at illumination intensities of the order of 10 to 100 milliwatts per square centimeter. Energy conversion efficiency versus illumination intensity is shown in Figure 2 for a silicon photovoltaic cell which is designated as a "ten percent solar cell". The illumination intensities given in this figure

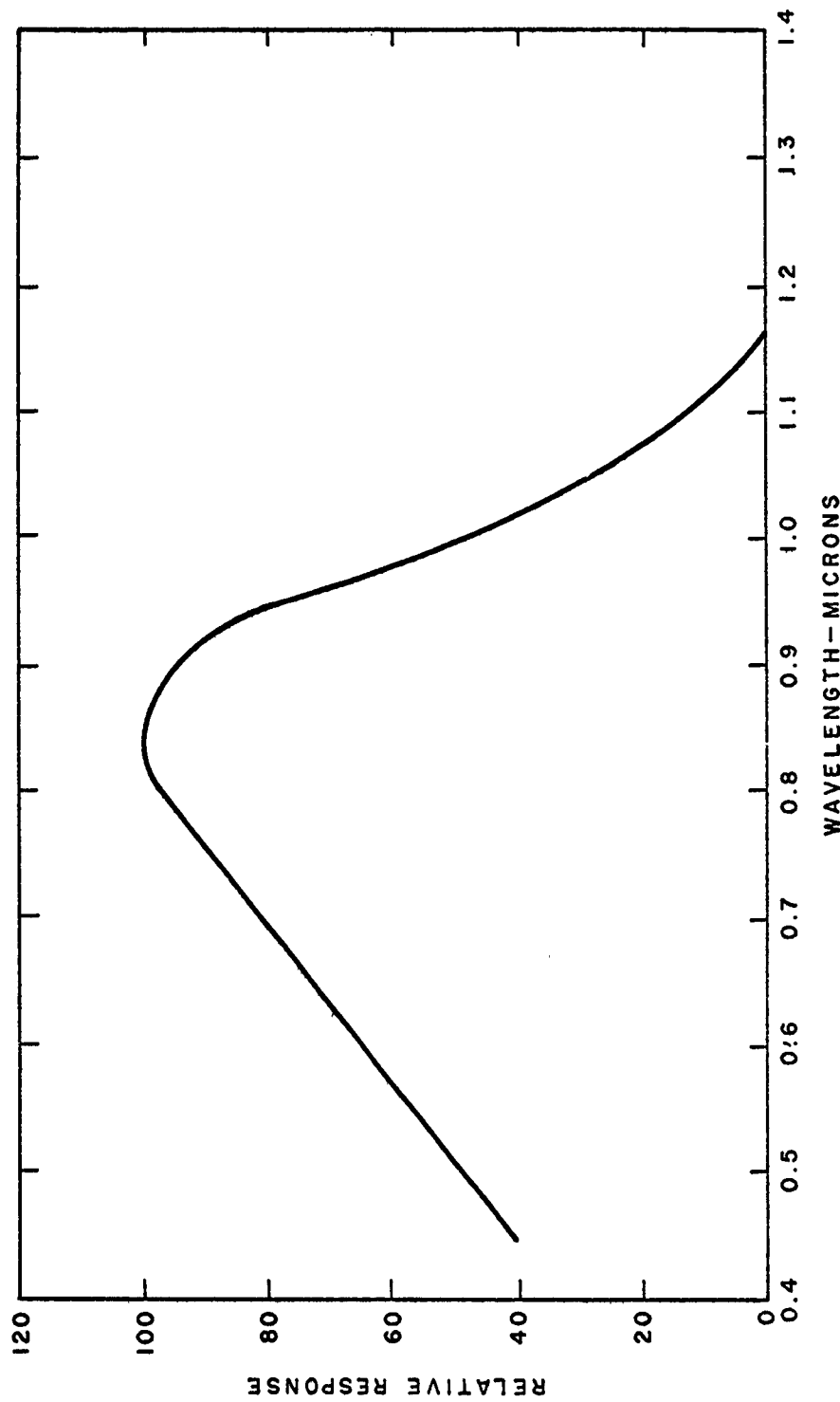


Figure 1

SPECTRAL RESPONSE OF SILICON P-n PHOTOVOLTAIC CELLS

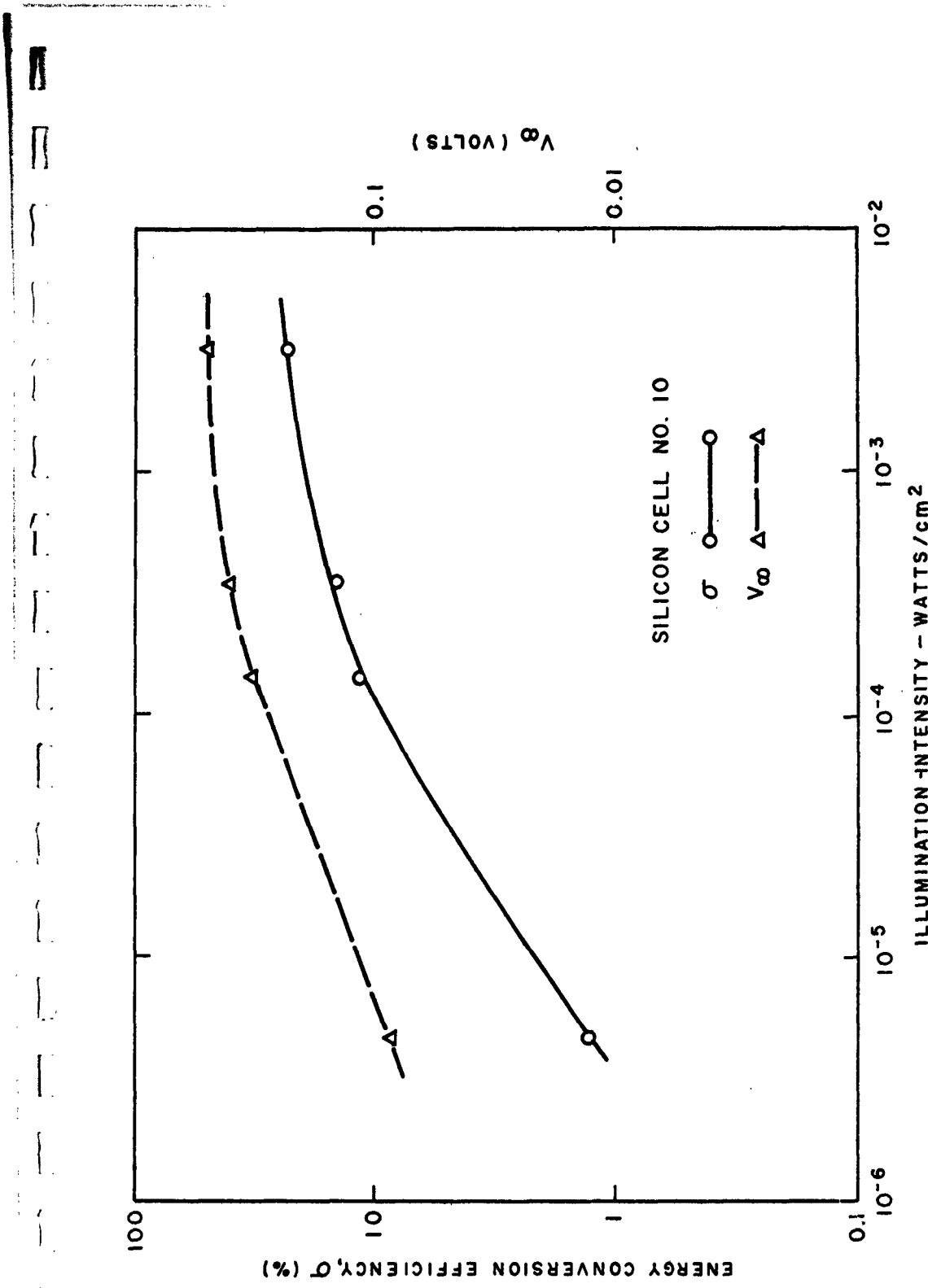


Figure 2
EFFECT OF ILLUMINATION INTENSITY ON THE ENERGY CONVERSION EFFICIENCY
AND OPEN CIRCUIT VOLTAGE OF A SILICON P-n PHOTOVOLTAIC CELL

are for photons between 590 millimicrons and 1.0 micron from a tungsten lamp. An Eppley thermopile was used to measure the output of a tungsten lamp which was filtered with both a sharp cut-off red filter transmitting wavelengths greater than 590 millimicrons and a water filter which absorbs the far infrared wavelengths above 2.4 microns. The radiant energy in the region between 1.0 to 2.4 microns was estimated and subtracted from the thermopile reading. Screen type neutral density filters were used to attenuate the illumination intensity. The conversion efficiencies quoted are at the maximum power points as determined from the i-V curves.

The photovoltaic cell voltage was measured with a Hewlett-Packard Model 425 A - DC microvoltmeter. This meter was used for all cell measurements in this reported work. Load resistances were obtained with a General Radio Type 602 M decade resistance box.

Silicon p-n photovoltaic cells were obtained for the purposes of determining the effects of nuclear radiation and temperature on conversion efficiency and to examine phosphor light outputs. All cells were checked for their conversion efficiency and shape of their i-V curves to insure that cells of similar or at least known characteristics were being used for the various studies.

Phosphors

Much of the success for the design of a high efficiency power source depends on the choice of the phosphor material. It must have a high energy conversion efficiency, be resistant to radiation damage, and emit in a region of maximum sensitivity for the photovoltaic device.

Many materials have been used to absorb nuclear radiation and emit photons. In general these materials may be divided into two large categories--organic and inorganic. For this application the use of organic phosphors is limited because of their instability at elevated temperatures and their low absorbing power for high energy charged particles. For the most part, inorganic phosphors have been found to be more efficient for nuclear excitation than organic phosphors.

Of the many inorganic phosphors, both simple and complex in structure, only those of the zinc sulfide group have been found practical for light sources under excitation by nuclear radiation (Ref. 4). Other inorganics are lower in conversion efficiency or are rapidly destroyed under the high level bombardment required. Energy conversion efficiencies of about 25 percent have been reported for ZnS type phosphors under nuclear particle excitation (Ref. 5). On the basis of the characteristic energy loss of electrons in zinc sulfide (17 ev) (Ref. 17), and since the average energy of the emitted photon is about 2.7 ev, it has been argued (Ref. 18, 19) that this conversion efficiency approaches the theoretical limit of cathodoluminescence efficiency of ZnS. The maximum conversion efficiencies for ZnCdS: Cu phosphors in cathodoluminescence (10-20 kev electron excitation) occurs at power input densities of about 2.5 microwatts per milligram of phosphor (Ref. 20). Increasing the power input decreases the conversion efficiency for this type phosphor.

Table 2 shows the emission peak and energy conversion efficiency of several members of this family. Although only one zinc-cadmium sulfide is shown, in all cases the emission spectra shift to the red as more cadmium is added. Since silicon has been chosen as the best photovoltaic material at the present time, it is desirable to choose one of these ZnCdS phosphors that emit near the peak of the silicon sensitivity. Pure cadmium sulfide activated with silver or copper has the lowest energy emission peak of any phosphor in this family and thus, on this basis, it is the most satisfactory phosphor. The choice of activator will depend on the relative efficiency observed with each.

The relative luminescence outputs of various powdered phosphors were measured. The phosphors examined included several which were in our laboratory for other purposes and some unknown, i. e. identified only by name or code number, "red" emitting phosphors. This initial phosphor scanning was performed using ultraviolet excitation and a silicon cell detector. Relative light outputs per unit area of phosphor are given in Table 3. A sharp cut-off filter which is transparent at wavelengths greater than 0.59 microns was used to determine how much of the luminescence is in the spectral region of maximum efficiency of the silicon. This is indicated in the table by the ratio of $L(\text{red})$ to $L(\text{total})$. It must be noted, however, that the silicon detector response cuts off above 1.0 micron, and thus a material such as CdS: Cu whose emission band is entirely above 0.59 microns ($L(\text{red})/L(\text{total}) = 1.0$) may give a low light output reading because of response losses at the longer wavelengths.

The best response to a silicon cell was observed from the (0.6) Zn (0.4) CdS: Cu phosphor. Differences in the useable light outputs of the various ZnCdS: Cu phosphors were not great. It is interesting that the ZnS: Cu phosphors exhibited a very good response to the silicon cell even though but a small fraction of their light output was in the wavelength region above 0.59 microns. The NBS 1024 standard phosphor was given the relative light output value of 100 simply because this was one of the first phosphors available in this study. This phosphor was used for the source-phosphor mix study and this phosphor and several others were examined for other characteristics pertinent to their use in a power source.

The phosphor may be in either of two forms - a large single crystal or a small particle polycrystalline powder mass. When using high energy beta particle excitation the optical transparency of the phosphor to its own emission is a critical factor. The single crystal phosphor has the advantage of a much higher optical transparency than the powder mass. All of the phosphors listed in Table 3 were powders; however, we obtained several samples of single crystal cadmium sulfide with various dopants with the hope that we would have a good red luminescent material of single crystal form. None of the samples was useable.

Table 2

EMISSION PEAK AND ENERGY YIELD OF SEVERAL ZINC SULFIDE TYPE PHOSPHORS EXCITED BY NUCLEAR RADIATION

	<u>Emission Peak</u> <u>λ (mμ)</u>	<u>E(ev)</u>	<u>Energy Yield^(a)</u> <u>α-exc.</u>	<u>β-exc.</u>
ZnS:Ag	437 ^(b)	2.84	.28	.14
ZnS:Cu	445 ^(b)	2.79	.25	.23
(0.4)Zn(0.6)CdS:(Ag)	590 ^(b)	2.1	-	-
CdS:Ag	730 ^(c)	1.7	.22	.16
CdS:Cu	820 ^(b)	1.51	-	-

(a) Miller, C. G., et. al., "Radioisotope Use for Self-Luminous Highway Directional Signs," U.S. Nuclear Corp., Quarterly Progress Report June 1 - August 31, 1961, USNC 61-103.

(b) Payen de la Garanderie, H., "Emission Spectra of Mixed Zinc and Cadmium Sulfides Activated by Silver: Existence of Two Emission Bands," J. Phys. Radium 22, 428 (1961).

(c) Grillot, E., "Comparative Study of Silver and Copper Luminescence Centers in Zinc Sulfide and Cadmium Sulfide Luminophors," J. Phys. Rad. 17, 624 (1956).

Table 3

**RELATIVE LIGHT OUTPUT, L, PER UNIT AREA
OF VARIOUS PHOSPHORS UNDER ULTRAVIOLET EXCITATION
AS DETECTED BY A SILICON PHOTOVOLTAIC CELL**

<u>Phosphor No.</u>	<u>Phosphor Type</u>	<u>L</u>	<u>L(red)/L(total)</u>
US Radium-S. O. *	(0.6)Zn(0.4)CdS:Cu	124	0.907
US Radium-S. O. *	ZnS:Cu	115	0.063
US Radium-S. O. *	(0.8)Zn(0.2)CdS:Cu	113	0.445
US Radium-S. O.	(0.4)Zn(0.6)CdS:Cu	107	0.915
NBS 1024	ZnCdS:Cu	100	0.500
Sylvania-146(P-14)	ZnCdS:Cu	95	0.513
Sylvania 140(P-7)	ZnCdS:Cu	83	0.231
Sylvania 110	ZnCdS:Ag	83	0.875
NBS 1022	ZnS:Cu	80	0.072
US Radium-S. O. *	(0.2)Zn(0.8)CdS:Cu	66	0.932
US Radium 4981	—	49	0.06
US Radium 4647	—	47	0.074
US Radium 4985	—	46	0.078
Iraser 6	—	43	0.050
US Radium 4890	—	37	0.146
US Radium 4989	—	35	0.085
Sylvania P-11	ZnS:Ag	35	0.08
NBS 1020	ZnS:Ag	33	0.08
Sylvania 211(P-13)	MgSiO ₃ :Mn	24	0.0
Iraser 2	—	21	0.12
US Radium-S. O. *	CdS:Cu	17	1.00
Sylvania 151	Zn ₃ (PO ₄) ₂ :Mn	12	0.26
Iraser 1	—	8	0.09
NBS 1025	Zn ₃ (PO ₄) ₂ :Mn	7	0.20
Iraser 8	—	6	0.33
Iraser 7	—	5	0.17
Iraser 3	—	4	0.33

* S. O. = Special Order

The cadmium sulfide single crystal samples examined were:

CdS - pure
CdS:Ag (unknown concentration)
CdS: CuCl₂ (unknown concentration)
CdS:Cu (lightly doped)
CdS:Cu (25 ppm)
CdS:Cu (75 ppm)
CdS:In (20 ppm), Ag (40 ppm)

By their optical appearances it is certain that the samples with unknown dopant concentrations had appreciably less doping than the last three samples on the list. We made a few attempts to diffuse silver and copper into the pure CdS samples but none of these trials produced a luminescent material. All samples were checked with both ultraviolet excitation and strontium-90 beta excitation, and no luminescence was detected either by eye or by a silicon cell or a multiplier phototube. The most promising samples are the more heavily doped materials (the last three in the list). Small regions in the large pieces of these materials and flakes and needles which are broken off of a large piece do exhibit a bright red luminescence. The bulk of the piece, however, does not luminesce.

There are but a few literature references on luminescent large crystal CdS (Ref. 21, 22, 23). A recent reference (Ref. 22) indicates that nonuniform luminescent properties were found in large pieces of cadmium sulfide.

NUCLEAR RADIATION EFFECTS

Two silicon p-n junction photovoltaic cells were irradiated with cobalt-60 gamma rays (1.17 and 1.33 MEV) at an intensity of 10^4 rads per hour. The cells were given radiation doses from 10^2 to 2×10^6 rads in several steps, and their conversion efficiency was determined after each dose increment. The decrease in efficiency with increased radiation dose is shown in Figure 3. Both cells showed identical behavior with both filtered and unfiltered tungsten light. After the complete irradiation, one cell was heated to 100°C for six hours to see if some of the original properties would return by temperature annealing. It was observed that there was a further drop of 30 percent in efficiency. Additional heating produced no further effect.

Three phosphors were also irradiated with cobalt-60 gammas at a dose rate of 10^6 rads per hour. The relative efficiency of these phosphors was checked at various dose increments with strontium-90 beta excitation. One of these phosphors, Sylvania 110 (ZnCdS:Ag), had such a low efficiency initially that the error of readability masked any observable changes. The other two phosphors, NBS 1024 (ZnCdS: Cu) and (0.6)Zn(0.4)CdS: Cu, exhibited the same behavior - a drop in efficiency beginning at about 10^7 rads with a decrease to 50 percent at 10^9 rads. The data for the NBS 1024 phosphor are plotted in Figure 3. Annealing the irradiated phosphors at 100°C for 16 hours produced a 15 percent recovery in light intensity; further annealing at 150°C for 16 hours gave an additional 10 percent recovery.

A 160 mg/cm² thickness of the NBS 1024 phosphor powder was given a continuous irradiation for 1000 hours by a sealed strontium-90 beta source of 0.3 curie intensity.⁵ The beta particle energy deposition rate in this phosphor was 3.2×10^5 ergs/cm² hr. as determined by cobalt glass dosimetry. The luminescence output for this beta excitation was measured with a silicon cell at various times during the irradiation. In this experiment, the silicon cell is inserted for measurement for only a short time so that there is no radiation effect upon the detector.

After 1000 hours of beta irradiation there was less than a 10 percent decrease in light output (Note: the data reported in ARF 1214-TR3, p. 17, January 15, 1963, where a light output decrease to 80 percent was given for 800 hours of beta irradiation, was found to be in error due to faulty silicon cell readings). The total energy dose would be 3.2×10^8 ergs/cm² in 160 mg/cm², or using the conversion 100 ergs/gm = 1 rad this dose is roughly equivalent to 2×10^7 rads. It would appear then that the strontium-90 beta was no more damaging than cobalt-60 gammas, and thus the cobalt-60 radiation effects are indicative of the damage expected with a high energy beta particle irradiation.

The sealed strontium-90 beta source used was a low intensity source. The power excitation rate from this source is about $10 \mu\text{w}/\text{cm}^2$ in the phosphor or an average phosphor excitation of about $0.06 \mu\text{w}/\text{mg}$. One would expect to operate at powers of one hundred times this number. At this higher power density the onset of radiation damage would be noticeable after 10 to 100 hours of operation.

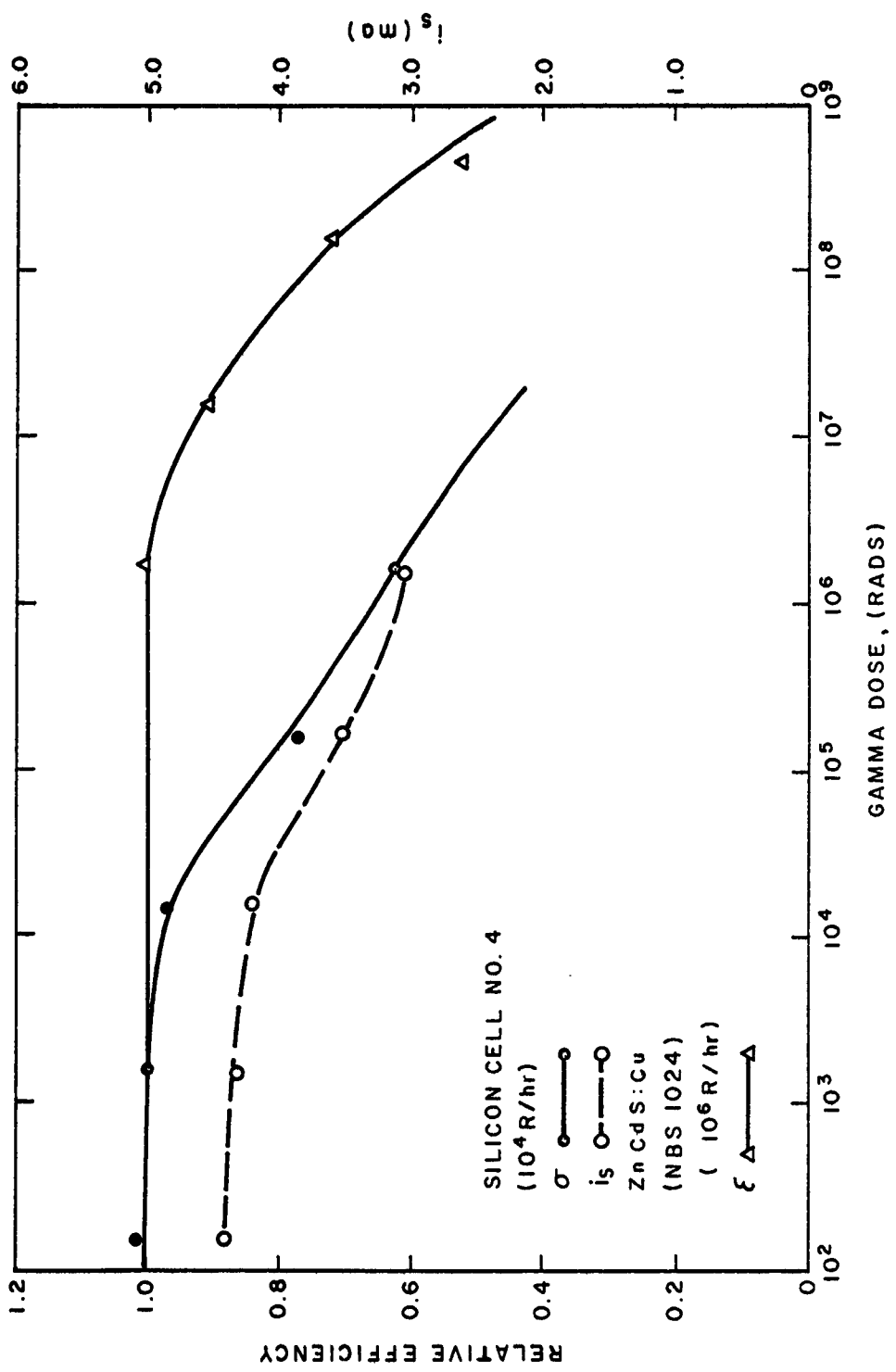


Figure 3
EFFECT OF COBALT-60 GAMMA RADIATION ON THE RELATIVE EFFICIENCIES OF A ZnCdS:Cu PHOSPHOR AND A SILICON p-n PHOTOVOLTAIC CELL

Low energy betas from promethium-147 (0.22 Mev max.) are reported not to be damaging to the phosphors used in high brightness nuclear light sources (Ref. 4, 5, 6). Several mixes of promethium-147 and ZnCdS:Cu have been prepared during this program (see section on Source-Phosphor Geometry) with total input power densities of about $10 \mu\text{w}/\text{mg}$ of phosphor. These mixes have retained their initial light output for over 1000 hours of operation to date.

All of the beta particle energy should be expended within the phosphor. The photovoltaic converter should not see the direct beta excitation, but it will be irradiated by bremsstrahlung. As mentioned earlier, the bremsstrahlung dose rate in a strontium-90 fueled power source using multi kilocuries would be at least 10^5 rads per hour at an average gamma energy of about 236 kev. This radiation would cause an onset of damage to a silicon p-n cell at 10 to 100 hours. The threshold electron energy for damage in such a cell is reported as 145 kev (Ref. 24). A n-p junction silicon cell is reported to withstand at least an order of magnitude more radiation for similar damage (Ref. 25). The low intensity and low energy (~ 20 kev) bremsstrahlung from promethium-147 should not seriously affect the life of a silicon photovoltaic cell.

We tried to obtain a n-p silicon cell during this project from a commercial source. Unfortunately, even after a second request, we never received the cell.

It is apparent that the damage, and also the shielding that would be required, accompanying multi kilocurie amounts of strontium-90 prohibit its use in such a power source.

TEMPERATURE EFFECTS

An appreciable amount of the input energy of the double conversion power source will be dissipated as heat. At equilibrium, the power source will have a constant temperature, depending on the power input, efficiency, and physical configuration. In order to design the 10 watt generator, it is necessary to know the effect of temperature on the components of the power source, so that provisions may be made for the required amount of heat dissipation. For this reason, the effect of increased temperature on the efficiency of silicon cells and various phosphors was studied.

Temperature Effect on Efficiency

For determining the effect of temperature on the silicon cell, a copper block with a deep slot for the silicon cell and a hole for a thermometer was constructed. This was then placed on a laboratory hot plate and the light source suspended from above. The thermometer hole was filled with glycerol to ensure good heat transfer; also stem temperature corrections were made. No time lag was observed between the increase in temperature as read on the thermometer and the decrease in power output of the solar cell. Upon cooling, the solar cell regained its original characteristics. A prolonged heating test was made on the same cell for 6 hours at 110°C with no detectable change in characteristics upon cooling. The curves of the relative efficiency and V_o versus T at constant illumination intensity for a silicon cell are shown in Figure 4.

The temperature dependence of the luminescence intensity under constant ultraviolet excitation was experimentally determined for the following phosphors: ZnCdS: Cu (NBS 1024), ZnS: Cu (NBS 1022), ZnS: Ag (NBS 1020) and U. S. Radium 4890 powder phosphors. The ZnCdS: Cu and ZnS: Cu phosphors were examined since they have produced the best response with silicon cells; the ZnS: Ag was examined to check the difference between a copper and silver activated phosphor; and the US Radium 4890 was examined since it has a greater proportion of emission in the red end of the spectrum than any other phosphor of significant emission except for the ZnCdS: Cu. (See Table 3)

A modified laboratory hot plate was used to heat the phosphor, whose temperature was measured with a thermocouple. Each temperature point was allowed to come to equilibrium. Luminescence was measured with a silicon cell both with and without an optical filter which passes light of wavelength greater than 0.59 microns. A water filter was used in front of the silicon detector to reduce the heat radiation to the detector. The detector was removed between readings to prevent it from heating up. A complete temperature run was made with a "dummy" sample, during which time the detector was checked with constant illumination and the detector sensitivity remained constant.

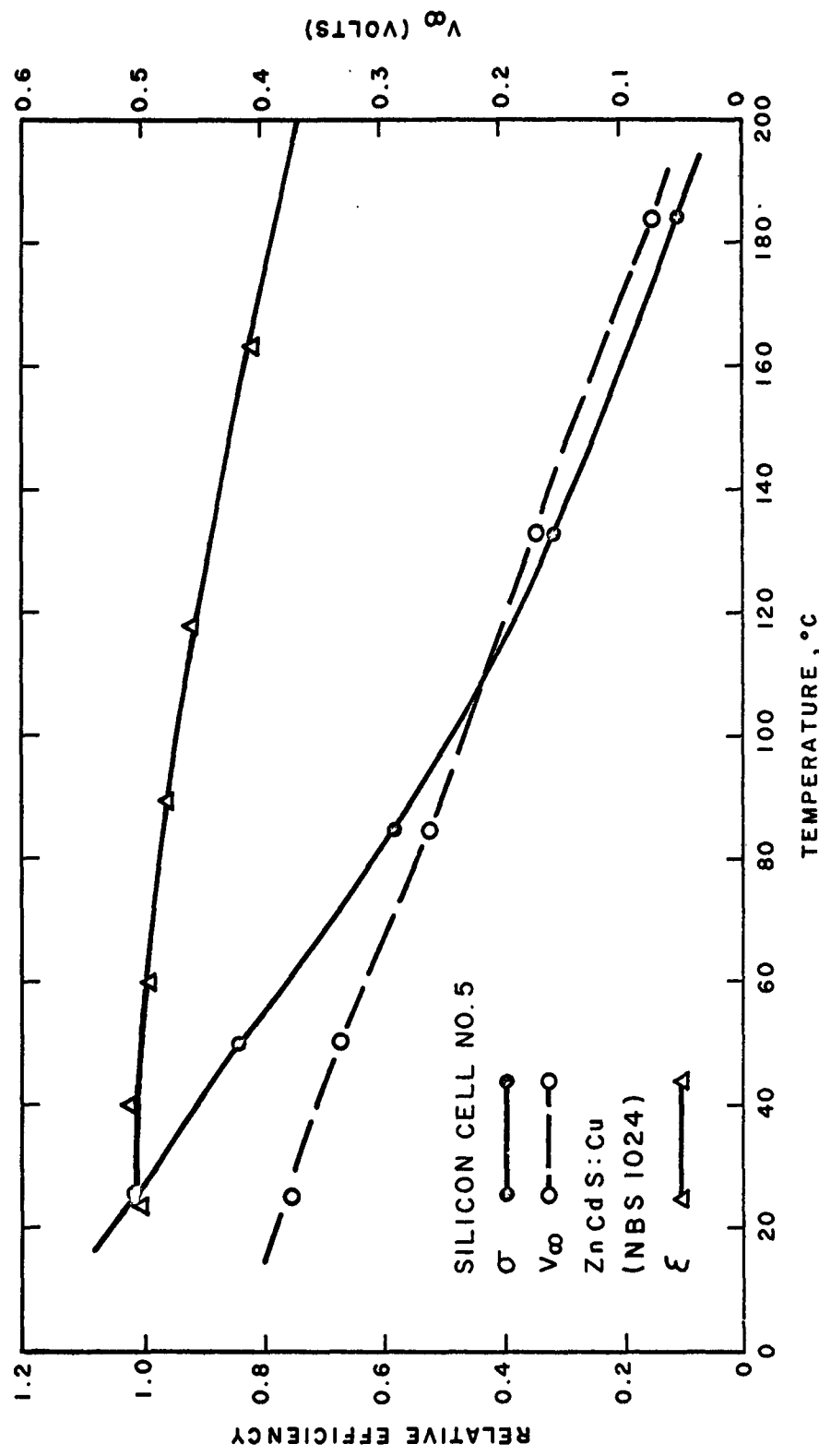


Figure 4
EFFECT OF TEMPERATURE ON THE RELATIVE EFFICIENCIES
OF A ZnCdS: Cu PHOSPHOR AND A SILICON p-n PHOTOVOLTAIC CELL

Temperature data are shown in Figures 4 and 5. Phosphor efficiency is given relative to a normalized value of 1.0 at room temperature for all cases. The ZnS: Cu and ZnCdS: Cu phosphors retain a useable luminescence up to temperatures of about 150°C. It was observed in all cases that the relative amount of luminescence passing through the red transmitting filter increased as the temperature increased.

The ZnS: Ag phosphor shows an appreciable decrease in light output with increased temperatures. US Radium 4890, not shown here, was completely quenched at a temperature of 100°C. This temperature behavior for a silver activated phosphor versus a copper activated phosphor is also reported in Leverenz (Ref. 20) for several of the ZnS-CdS type phosphors. Thus for this program the copper activated phosphors appear to be the most useable.

From Figure 4 it is apparent that, although the efficiency of both the silicon cell and the ZnCdS: Cu decrease as temperature increases, the maximum permissible temperature is more influenced by the silicon cell than the phosphor. A maximum temperature of 100°C, where the total efficiency is at 50 percent of its room temperature value, has been chosen for power source design discussion.

Temperature Restriction on Power Source Geometry

Consider each unit power cell as being composed of a source-phosphor combination sandwiched between two photovoltaic converters. The limitation of the source-phosphor combination thickness is governed primarily by the optical properties of the phosphor, as discussed elsewhere in this report. The maximum number of unit cells which may then be stacked, surface to surface, without reaching a temperature greater than 100°C in the center of the stack has been calculated for a mixture of powdered promethium oxide (Pm_2O_3) and powdered ZnCdS: Cu phosphor with a total thickness of 85 mg/cm^2 between two silicon cells, each of thickness 130 mg/cm^2 . The activity contained in this unit is about 4 curies/ cm^2 or about 1.52 mw/cm^2 . The method of heat transfer considered is radiation to black space from the ends of a stack of units. The details of the calculation are given in Appendix I.

For radiative cooling to black space, the maximum permissible number of units which may be stacked without exceeding a temperature of 100°C was calculated as 140 units in the mixed source phosphor device. This corresponds to a total input power per stack of 214 mw/cm^2 . Assuming an overall conversion efficiency of one percent, this would produce an output power of 2.14 mw/cm^2 of stacked units. Then, for 10 watts total output power, a stack area of 4630 cm^2 is required.

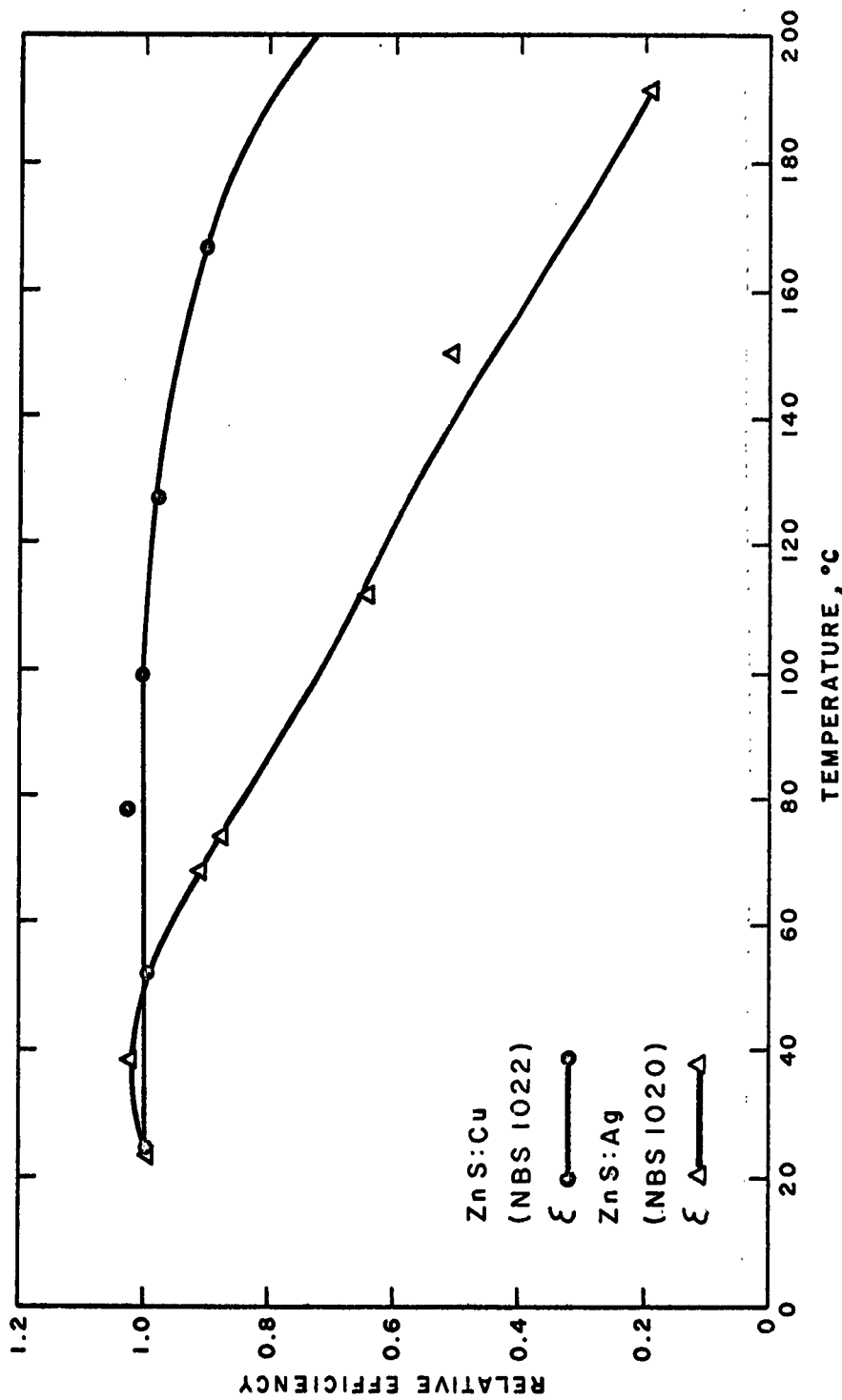


Figure 5

EFFECT OF TEMPERATURE ON THE RELATIVE EFFICIENCIES
OF ZnS: Cu AND ZnS:Ag PHOSPHORS

SOURCE-PHOSPHOR GEOMETRY

Back Surface Beta Excitation

One method of producing light with a phosphor and beta particle radiation is to place the radioisotope on one side or surface of a phosphor mass. Both the beta particle range and the optical transparency of the phosphor determine the light output in this geometry. Calculations were made on the relative light output from phosphors in both a powdered and a transparent crystal form. It is assumed that the phosphor obeys Lambert's law for the absorption of its own emitted radiation, that is the decrease in intensity with distance is proportional to the intensity. The exciting beta radiation is considered to be absorbed exponentially by the phosphor for a radiation source behind the phosphor. The derivation of the equation for the light output of the phosphor is as follows:

$$\frac{dL(x)}{dx} = \lambda I(x) - \epsilon L(x) \quad (1)$$

$$I = I_0 e^{-\mu x} \quad (2)$$

where

$L(x)$ = light output

x = distance in phosphor (mg/cm^2)

λ = conversion efficiency of exciting beta radiation into light ($\text{light energy}/\text{cm}^2$)

$I(x)$ = intensity of beta radiation as a function of x

I_0 = intensity of beta radiation at $x = 0$

μ = absorption coefficient of the beta radiation in the phosphor (cm^2/gm) (for Sr^{90} , $\mu = 6.8 \text{ cm}^2/\text{mg}$) (Ref. 13)

ϵ = absorption coefficient of the emitted photon radiation in the phosphor (cm^2/gm).

Thus

$$\frac{dL(x)}{dx} = \lambda I_0 e^{-\mu x} - \epsilon L(x) \quad (3)$$

The solution of this first order linear differential equation is, (see for example, "Advanced Engineering Mathematics" by C. R. Wylie, pp. 11-13 (McGraw Hill Book Co.),

$$L(x) = \frac{\lambda I_0}{\epsilon - \mu} e^{-\mu x} + C e^{-\epsilon x}. \quad (4)$$

At $x = 0, L(0) = 0$
 so that $C = \frac{-\lambda I_0}{\epsilon - \mu}$
 and $L(x)/I_0 = \frac{\lambda}{\epsilon - \mu} (e^{-\mu x} - e^{-\epsilon x}). \quad (5)$

The derived formula assumes that the intensity of beta particles through the phosphor decreases exponentially, which is a good approximation up to one-half the range. At least 80 percent of the beta particles are stopped in this thickness. As a corollary to this, one may use a phosphor thickness one-half the range of the beta particles with little loss in light output in the transparent phosphors.

The effect of phosphor optical half thickness or absorption coefficient on the light output from a back surface Sr-90 excited phosphor was then calculated. The results of this calculation are summarized in Table 4.

A study of back surface Sr-90 excitation of several phosphors was also made experimentally. The phosphor container used for these measurements is shown in Figure 6. It consists of a brass cylinder 1-1/2 inches in diameter with a 1 inch hole through the center. A small lip on the lower edge of the hole allows the insertion of a thin (30 mil) piece of fused silica. This fused silica, Corning 7940, has been reported to be extremely resistant to radiation coloring. A layer of phosphor powder of various thicknesses or a single crystal of phosphor is then inserted into the cylinder. A second piece of fused silica is followed by a cork gasket and a hollow brass plug which may be screwed to the bottom piece. For beta particle excitation, the top piece of fused silica is removed.

To use an existing strontium-90 source for phosphor excitation and radiation damage studies, it was necessary to design a container which would permit maximum utilization of the beta particles from the source while minimizing personnel radiation exposure from both the beta particles and bremsstrahlung. The Sr-90 itself is a thin disc about 3/8 inch in diameter held in a brass disc about 1/2 inch thick and with a 1 inch diameter. The holder for the source, shown in Figure 7, is a steel cylinder six inches in diameter and 3-1/2 inches thick with a hole in it allowing the source to be placed inside. A brass cover plate is then placed over the source to hold it in position. This cover plate is equipped with spring loaded tracks so that a drawer containing the materials to be examined may be inserted. The drawer is equipped to carry the brass phosphor container, described above, and a silicon cell. Electrical connections for the silicon cell are made by a pair of insulated copper leaf spring terminals on the drawer and two insulated copper blocks on the brass cover plate. From the connections on the cover plate, leads are attached to a standard coaxial connector on the top of the steel cylinder.

Table 4
 CALCULATED RELATIVE LIGHT OUTPUT
 FOR BACK-SURFACE Sr^{90} EXCITED PHOSPHORS
 OF VARIOUS TRANSPARENCIES

Optical Half Value Thickness (mg/cm ²)	ϵ (cm ² /g)	Optimum Thickness (mg/cm ²)	$L(x)/I_o \lambda$
20	34.6	58.5	.019
69.3	10.0	120.	.044
150.	4.62	175.	.064
300.	2.3	241.	.084
600.	1.15	315.	.103
1000.	.693	373.	.113
1500.	.462	425.	.121
∞	0	—	.147

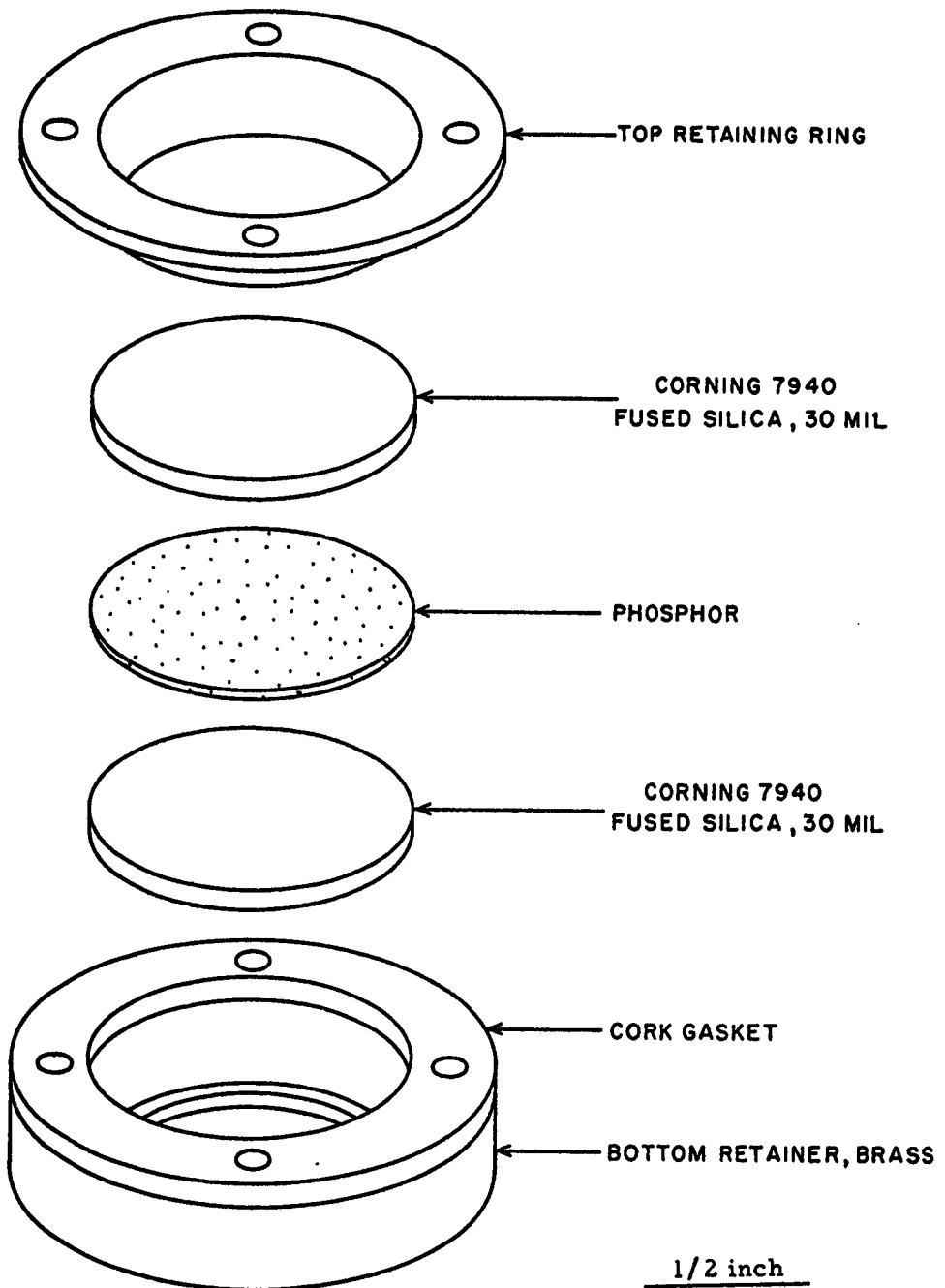


Figure 6
PHOSPHOR CONTAINER



Figure 7

STRONTIUM-90 BETA SOURCE HOLDER AND SAMPLE DRAWER

The distance from the surface of the beta source to the phosphor is about 1/2 inch and from the phosphor to the solar cell is about 1/8 inch. The total beta particle dose rate at the phosphor position, measured using cobalt glass dosimetry, is 6.0×10^5 ergs/cm² hr. Bremsstrahlung radiation at the sample position is 10 r/hr and at the surface of the steel shielding cylinder about 10 mr/hr.

Five different powdered phosphors have been examined to determine the light output versus thickness for back surface Sr-90 beta excitation. The data curves of relative light output as detected by a silicon cell versus phosphor thickness are shown in Figure 8 for several phosphors. Maximum light outputs are observed at 200 mg/cm² for (0.6)Zn(0.4)CdS: Cu, at 170 mg/cm² for ZnCdS: Cu (NBS 1024), at 150 mg/cm² for (0.4) Zn (0.6) CdS: Cu, at 110 mg/cm² for ZnS: Cu (NBS 1022), and at 30 mg/cm² for ZnS: Ag (NBS 1020). The optical half value thicknesses of these phosphors were calculated from these data, and they are:

(0.6)Zn(0.4)CdS: Cu	200 mg/cm ²
ZnCdS: Cu (NBS 1024)	150 mg/cm ²
(0.4)Zn(0.6)CdS: Cu	110 mg/cm ²
ZnS: Cu (NBS 1022)	60 mg/cm ²
ZnS: Ag (NBS 1020)	10 mg/cm ²

It was observed that calculated thickness versus intensity curves fit the measured data very well. The most promising powder phosphors for this application, the ZnCdS: Cu phosphors, have good transparencies to their own emission.

The beta excitation power from thick, semi-infinite, beta sources can be estimated by using the rule that the emergent energy from a surface of the source is equal to one-eighth of the total beta energy contained in the source volume whose thickness is equal to the range of the average energy beta particle (Ref. 26). This calculation was made for Pm-147, Tl-204, and Sr-90 using the theoretical maximum specific activities of Pm_2O_3 , metallic or elemental thallium, and SrTiO_3 as given in Table 1. Then the average excitation density in the phosphor can be estimated by assuming that the source output energy is all absorbed in a phosphor thickness equal to one-half the range of the maximum beta particle energy. The power out, the one-half ranges, and the phosphor excitation densities are respectively:

Pm_2O_3	; 310 $\mu\text{w}/\text{cm}^2$; 28 mg/cm ²	; 11 $\mu\text{w}/\text{mg}$
Tl	; 5470 $\mu\text{w}/\text{cm}^2$; 140 mg/cm ²	; 39 $\mu\text{w}/\text{mg}$
SrTiO_3	; 15400 $\mu\text{w}/\text{cm}^2$; 550 mg/cm ²	; 28 $\mu\text{w}/\text{mg}$.

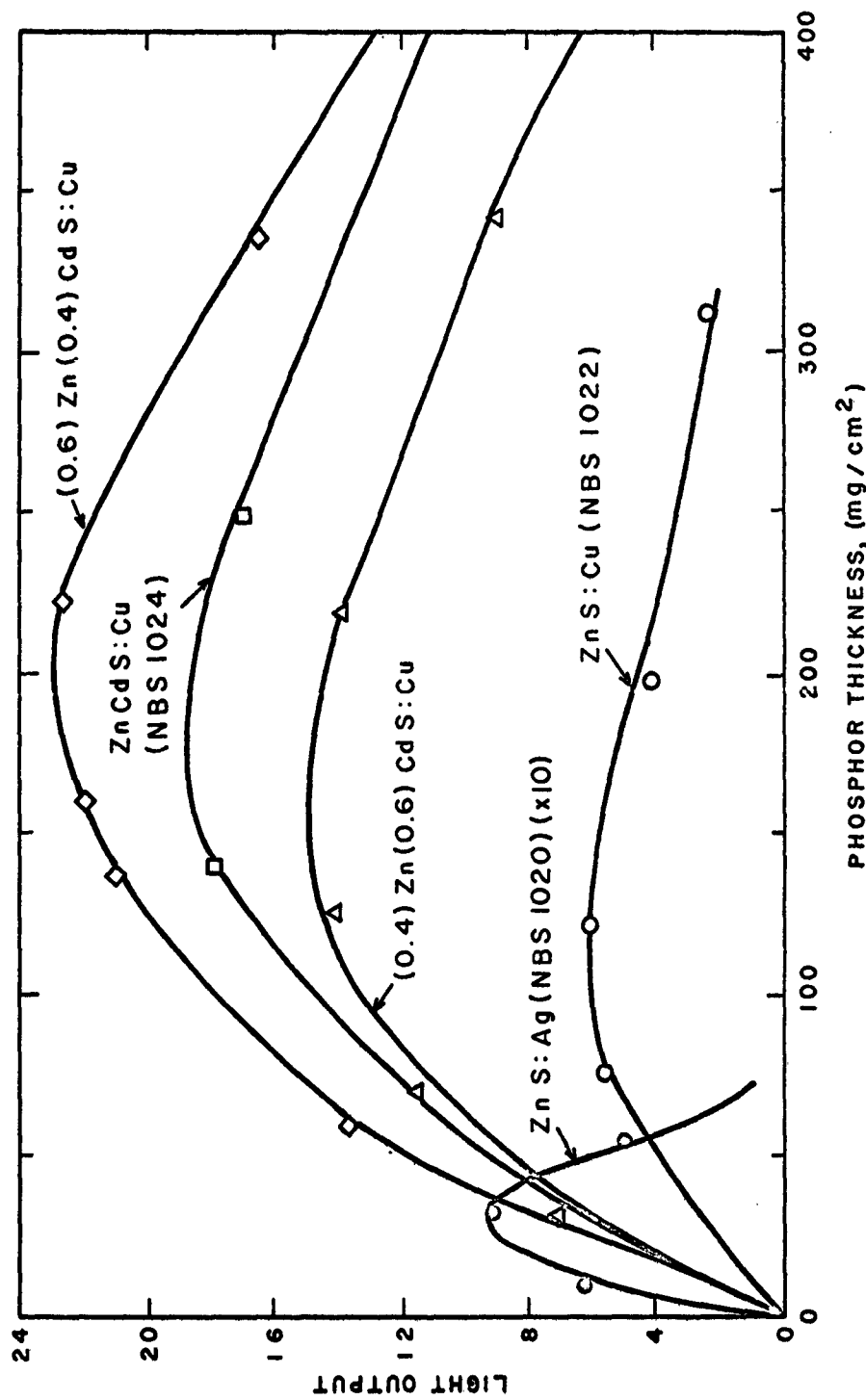


Figure 8

EFFECT OF PHOSPHOR THICKNESS ON LIGHT OUTPUT
WITH BACK-SURFACE STRONTIUM-90 BETA EXCITATION

Although the power outputs of the various maximum specific activity sources vary by orders of magnitude, the average phosphor excitation densities are practically equivalent. The optimum use of the sources is dependent upon matching the phosphor transparency and the beta range.

The measured light output from a 160 mg/cm^2 thickness of NBS 1024 phosphor excited by the experimental Sr-90 sources was $0.63 \mu\text{w/cm}^2$. The total power incident upon the phosphor was $6.0 \times 10^5 \text{ ergs/cm}^2 \cdot \text{hr}$ or $16.7 \mu\text{w/cm}^2$. Based on the incident beta power the light conversion efficiency is $0.63/16.7 = 0.038$ or 3.8 percent. Assuming a source efficiency of 12 percent, i. e. one-eighth of the total beta energy contained in the source emerges from one surface, the source-phosphor efficiency per source surface is $0.038 \times 0.12 = 0.0046$ or 0.46 percent. Since both surfaces of the source may be used for excitation, the total source-phosphor efficiency would be 0.92 percent.

Using thinner sources of high specific activity material would increase the total source-phosphor efficiency because of the reduced self absorption loss in the beta source. The resultant decrease in light output, however, would cause a decrease in photovoltaic conversion efficiency and would probably decrease the power out per unit weight. An example of these effects is illustrated later when discussing the source-phosphor powder mix geometry. When powder phosphor thicknesses of tens of mg/cm^2 are used it has been observed that a back surface optical reflector increases the light output by only 10 percent or less. The beta absorption in a reflector would most likely cancel out this small gain in light output.

It is seen from Table 4 that to fully utilize the range of the Sr-90 betas, a phosphor optical half value thickness greater than 1500 mg/cm^2 is required. A large crystal form of phosphor is necessary to realize such an optical transparency. With the optimum transparency phosphor the light output would be 2.3 times that for the NBS 1024 phosphor (150 mg/cm^2). In this case the light output should increase to $1.45 \mu\text{w/cm}^2$ and the total source-phosphor efficiency would increase to 2.1 percent.

The Sr-90 source used for the above experiments was very low in intensity and there was a loss of about ninety percent of the emerging betas due to the one-half inch spacing between the source and the phosphor. Therefore, if a thick source of maximum specific activity were used and if the phosphor efficiency remained constant at the higher excitation power density, a light output of about $580 \mu\text{w/cm}^2$ could be expected from the NBS 1024 phosphor and a light output of $1300 \mu\text{w/cm}^2$ could be expected from an "ideal" transparent phosphor.

The above discussion concerning Sr-90 beta source excitation is rather academic since the use of Sr-90 in a ten watt output double conversion power device is not practical due to radiation damage and shielding requirements as mentioned previously. A beta emitter such as Tl-204 would be better suited to this geometry with the existing phosphors, but the low currently available specific activity of thallium makes it impractical for use at this time.

A low energy beta, such as the Pm-147 beta, limits the useable thickness of phosphor to a value less than that which the optical transparency of the phosphor would allow. A better source-phosphor geometry for Pm-147 is the powder mix geometry which is described in detail later in this report.

Matrix Distribution of Source in Large Crystal Phosphor

If a transparent large crystal phosphor were available, a method of utilizing an optical transparency greater than the beta range is a source loading geometry that would provide source surfaces throughout the bulk of the phosphor. Two geometries of beta source loading in a phosphor slab are illustrated in Figure 9. In case A, the beta source is loaded in holes drilled into the phosphor slab, and in case B, the source is placed in slots cut into the phosphor. In both cases the hole diameter or slot width, S, would be related to the range of the beta particle in the source material; the spacing between holes or slots, P, is related to the beta range in the phosphor material; and a thickness P of phosphor is left intact at the bottom of the slab to which the photovoltaic converter is attached. This layer of phosphor would insure that no direct betas get to the photovoltaic converter.

In case A there will be one hole per $(\sqrt{3}/2)(P + S)^2$ top surface area. Each hole has a surface area of πSh , where h is the depth of hole. Thus the ratio of hole surface to top surface is

$$\pi Sh / (\sqrt{3}/2)(P + S)^2$$

Choosing P and S to be equal to the beta ranges and assuming that the densities of source and phosphor are nearly the same, we have $P = S$, and the above ratio becomes

$$\pi Sh / 2 \cdot \sqrt{3} S^2$$

or $0.91 h/S.$

It is easily calculated that the top surface remaining is 0.775 of the original. Thus in the geometry the total source surface area available per unit area of phosphor is

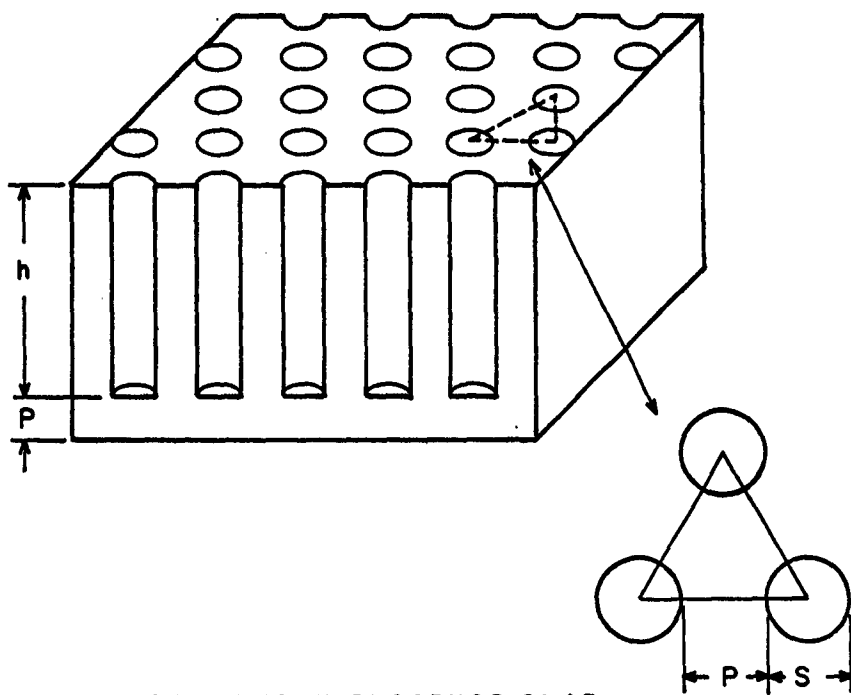
$$\text{source surface/unit area} = 0.775 + 0.91 h/S.$$

The phosphor volume to source volume ratio within the depth h is 3.44.

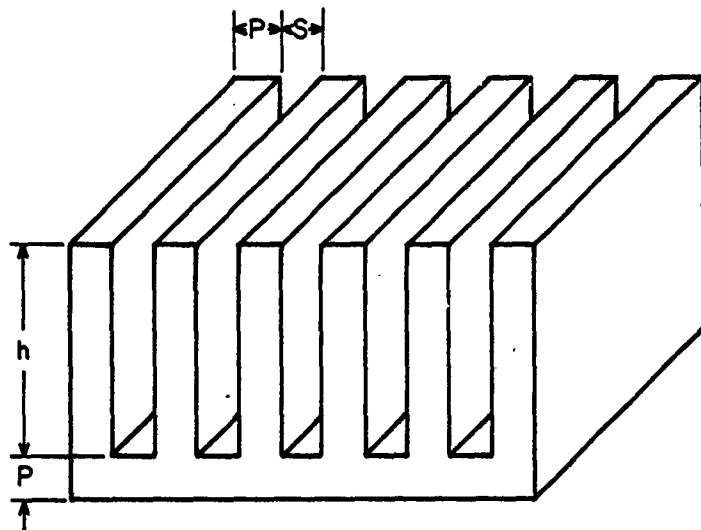
In case B the ratio of slot surface area to top surface is

$$2h (S + P) / (S + P)^2 = 2h / (S + P).$$

The phosphor volume to source volume ratio within the depth h is 1.0.



A. SOURCE HOLES IN PHOSPHOR SLAB



B. SOURCE SLOTS IN PHOSPHOR SLAB

Figure 9

GEOMETRY OF BETA SOURCE AND SINGLE CRYSTAL PHOSPHOR

Choosing P equal to the beta range in the phosphor is the condition for having essentially all of the phosphor material excited. To check the practicality of this condition consider the beta ranges in CdS, which has a density of 4.58 gm/cm³. These ranges are:

Pm-147	;	0.0125 cm.
Tl-204	;	0.0612 cm.
Sr-90	;	0.240 cm.

A spacing of 0.01 centimeters is not practical for fabrication. Probably one could consider using spacings of 0.1 centimeter or greater; thus Tl-204 and Sr-90 could be used most effectively in this geometry.

The depth h could be chosen, for example, to be equal to the optical half value thickness of the phosphor. None of the copper or silver doped large CdS crystals which we obtained were suitable luminescent materials, but we can infer from their optical transparencies what values of h may be practical. The copper doped CdS crystals had half value thickness for light at 800 millimicrons between 2.6 centimeters and 0.27 centimeters for "lightly" doped to 75 ppm of copper respectively. Assume then, that a value of 1.0 centimeter is practical for h . The source surface gain for a spacing of 0.1 centimeter is about 10, and for a spacing of 0.24 centimeters the source surface gain is greater than 4.0.

There would be light losses in the geometries of Figure 9 due to the source holes or slots. The lowest loss would be realized if the inside surfaces of the holes or slots were polished and cleaned with an air interface, i. e. the source material would not be in direct contact with the phosphor surfaces. Since CdS has a relatively high index of refraction (about 2.5) and thus a low critical angle for total internal reflection, the CdS phosphor would function well as a light pipe. A detailed analysis of the light collection has not been made for these slab geometries, although the light collection from luminescent fibers or rods has been studied (Ref. 27) and many of the considerations given to the cylindrical (rod) geometry would apply here.

It is believed that even with the light losses there would be a light intensity gain of two to four over the simple back surface excitation geometry. The source-phosphor efficiency would decrease, but since the photovoltaic conversion efficiency would increase it is possible that the overall efficiency may increase. This geometry requires experimental study which was not possible in this study program.

Source-Phosphor Powder Mix

Another type of source-phosphor geometry is that where a radioisotope source and a powder phosphor are intimately mixed together. The parameters of interest in this geometry are the phosphor mass per curie

of source and the total source-phosphor thickness for maximum light output. This geometry is most applicable for a low energy beta particle emitting isotope.

We used the ZnCdS: Cu powder phosphor (NBS 1024) and a processed high purity promethium-147 radioisotope. The radioisotope was obtained from Oak Ridge National Laboratory in the form of a promethium-147 oxide powder. The specific activity, based on the purity quoted by ORNL, is calculated to be about 680 curies per gram of oxide material on December, 1962. Samarium and neodymium oxides are the major impurities.

Enclosed containers, shown in Figure 10, were used for the source-phosphor mix study. These experimental containers are copper tubes which have been reamed out to have a one square centimeter inner cross sectional area. A radiation resistant fused silica (Corning 7940) window, also of one square centimeter area, is sealed at one end of each tube. A cylindrical steel piece is inserted inside the tube for the purpose of tamping the mixture and to serve as a back reflector. This tamper piece is controlled by a ring magnet which slips over the tube and allows one to raise and lower the tamper. The phosphor is added by a funnel through the side fill tube. When making additions the tamper is raised above the fill tube. The cylindrical boss above the fill tube is used for positioning the sample tubes.

Four experimental containers were loaded with 1.9 curies, 5.0 curies, 9.9 curies, and 16.7 curies of promethium oxide, respectively. Pre-weighed increments of ZnCdS: Cu phosphor powder were then added to the containers and the light output was detected with a silicon cell. The intensity measured after each phosphor addition to an individual tube may be plotted as a function of curies/cm² and mg of phosphor/curie. On each of these plots, a family of four curves is obtained, corresponding to the different containers. These raw data curves permit the determination of the amount of both source and phosphor required per unit area for maximum efficiency.

Table 5 summarizes the data obtained and the calculations performed on these data. Column B indicates the four source concentrations, with data for one curie/cm² extrapolated in a few cases. Column C is derived from Column B by the relationship 2600 curies of Pm₂O₃ corresponds to one watt.

The measured light intensity from the phosphor is shown in Column D. Column E then gives the source-phosphor efficiency. It can be seen that, regardless of the ratio of phosphor to source, the efficiency decreases as the amount of activity increases. This efficiency would approach an upper limit as the activity contained approaches zero. However, even though the efficiency decreases with higher concentrations of source, the light output increases. Since the efficiency of the silicon cell increases as the light increases, a maximum efficiency point for the whole system exists at a radioisotope concentration different from zero. Column F gives the measured efficiency of a high efficiency silicon cell at the various light intensities indicated in Column D. Multiplying Columns E and F gives the

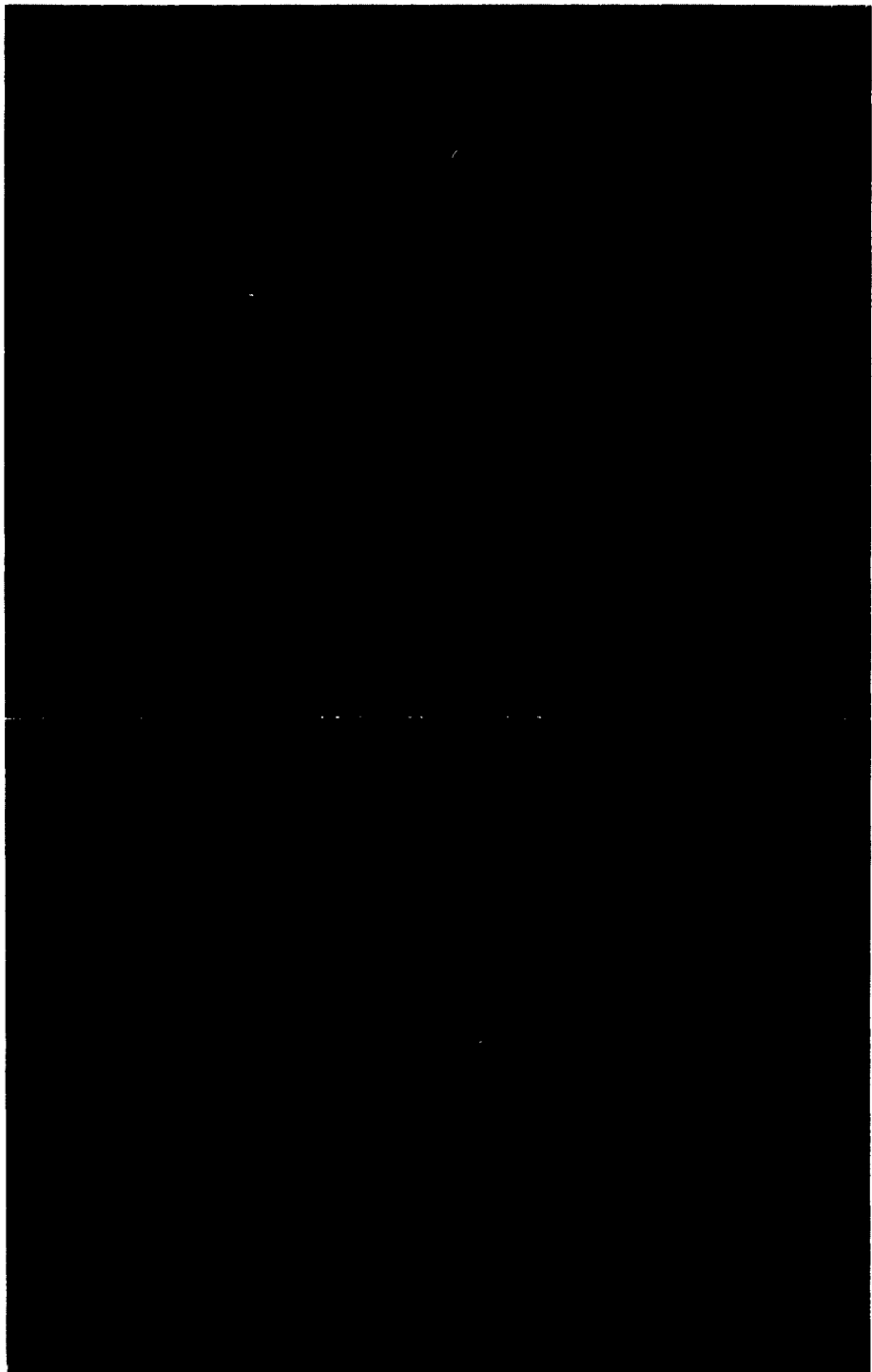


Figure 10

APPARATUS FOR CONTAINMENT AND EVALUATION
OF PHOSPHOR-SOURCE MIXTURES

Table 5
**EFFICIENCY DATA OF PHOSPHOR-SOURCE
 MIX AT VARIOUS LOADING RATIOS AND THICKNESSES**
 (Phosphor - ZnCdS:Cu (NBS 1024); Source - $\text{Pm}_2^{147}\text{O}_3$)

A	B	C	D	E=Dx'00/C	F	G=ExF/100
Phosphor- Source Ratio mg/curie	Source Loading curies/cm ²	Power Input mw/cm ²	Light Output μw/cm ²	Source- Phosphor Efficiency-%	Silicon Cell Efficiency-% (at illumin- ation "D")	Total Efficiency-%
5	1.	0.38	2.9	0.77	0.9	0.0069
	1.9	0.73	4.4	0.60	1.2	0.0075
	5.0	1.9	7.1	0.39	1.8	0.0072
	9.9	3.8	11.	0.30	2.3	0.0069
	16.7	6.4	14.	0.21	2.8	0.0023
10	1.	0.38	3.5	0.92	1.0	0.0097
	1.9	0.73	6.0	0.83	1.5	0.0129
	5.0	1.9	9.3	0.49	2.1	0.0103
	9.9	3.8	11.4	0.30	2.4	0.0072
	16.7	6.4	14.6	0.23	2.9	0.0067
15	1.	0.38	3.8	1.01	1.1	0.0111
	1.9	0.73	6.4	0.88	1.6	0.0141
	5.0	1.9	9.9	0.52	2.2	0.0115
	9.9	3.8	11.3	0.30	2.4	0.0072
	16.7	6.4	14.6	0.23	2.9	0.0067
20	1.	0.38	4.0	1.05	1.2	0.0126
	1.9	0.73	6.6	0.91	1.6	0.0150
	5.0	1.9	9.7	0.51	2.1	0.0110
	9.9	3.8	10.6	0.28	2.3	0.0065
	16.7	6.4	13.5	0.22	2.7	0.0060
28	1.	0.38	4.3	1.14	1.2	0.0139
	1.9	0.73	6.3	0.87	1.6	0.0140
	5.0	1.9	9.2	0.48	2.1	0.0098
	9.9	3.8	9.3	0.25	2.1	0.0053
	16.7	6.4	12.7	0.20	2.6	0.0052
40	1.9	0.73	6.2	0.85	1.6	0.0135
	5.0	1.9	7.4	0.39	1.7	0.0066
	9.9	3.8	8.2	0.22	1.9	0.0042

* All 1 curie/cm² data are extrapolated

total efficiency which may be expected from this type of power cell unit. These results are illustrated for a loading ratio of 20 mg/curie in Figure 11 where curves of source-phosphor efficiency, silicon cell efficiency, and total efficiency are plotted versus curies/cm². The total efficiency has a maximum point at about 2 curies/cm² for this phosphor to source loading ratio. The total efficiency as a function of source loading (curies/cm²) was plotted for the other phosphor-source ratios, and the maximum efficiency was determined for each ratio. These results are plotted in Figure 12 where it is observed that the efficiency shows a rapid rise and then a slow decrease as the loading ratio increases. A maximum efficiency occurs at about 20 mg/curie, which is a phosphor excitation density of 19 μ w/mg, or slightly less, since there will be some source self absorption in the mix.

The efficiency values listed in Table 5 are those obtained in the experimental conditions where the phosphor to photovoltaic cell coupling was not optimum, where only one side of the phosphor was used, and where both the phosphor and photovoltaic cell efficiencies could be improved slightly by using different materials. These improvements are accounted for in a later section describing a prototype power cell unit of the powder mix geometry. There it is shown that a total efficiency of 0.15 percent could be obtained.

Power Per Unit Weight Considerations

As indicated above, the maximum efficiency for a power cell unit using a source-phosphor mix of Pm_2O_3 and ZnCdS: Cu and a silicon photovoltaic converter occurs at a phosphor-source loading ratio of 20 mg/curie and at a source loading of 2 curies/cm². The standard silicon photovoltaic cells with contacts have a mass of 130 mg/cm². Each unit power cell would have two photovoltaic converters (one on each side of the source-phosphor mass). A maximum efficiency unit power cell is then composed of 260 mg/cm² of silicon and 40 mg/cm² of source-phosphor mix. The weight of Pm_2O_3 at 680 curies/gm is small (1.5 mg/curie) and can be neglected.

By working at a higher source loading the total efficiency drops, but both the light output and the power per unit area increase to a saturation value. Since the increase in source-phosphor mass is small compared to the mass of the silicon photovoltaic converters, the maximum power per unit weight in this case is not at the maximum efficiency.

The power per unit weight, P/M, is

$$P/M = \frac{C\epsilon}{(M_{pc} + M_{sp})}$$

where

C = source loading in curies/cm²

ϵ = total power conversion efficiency at source loading C

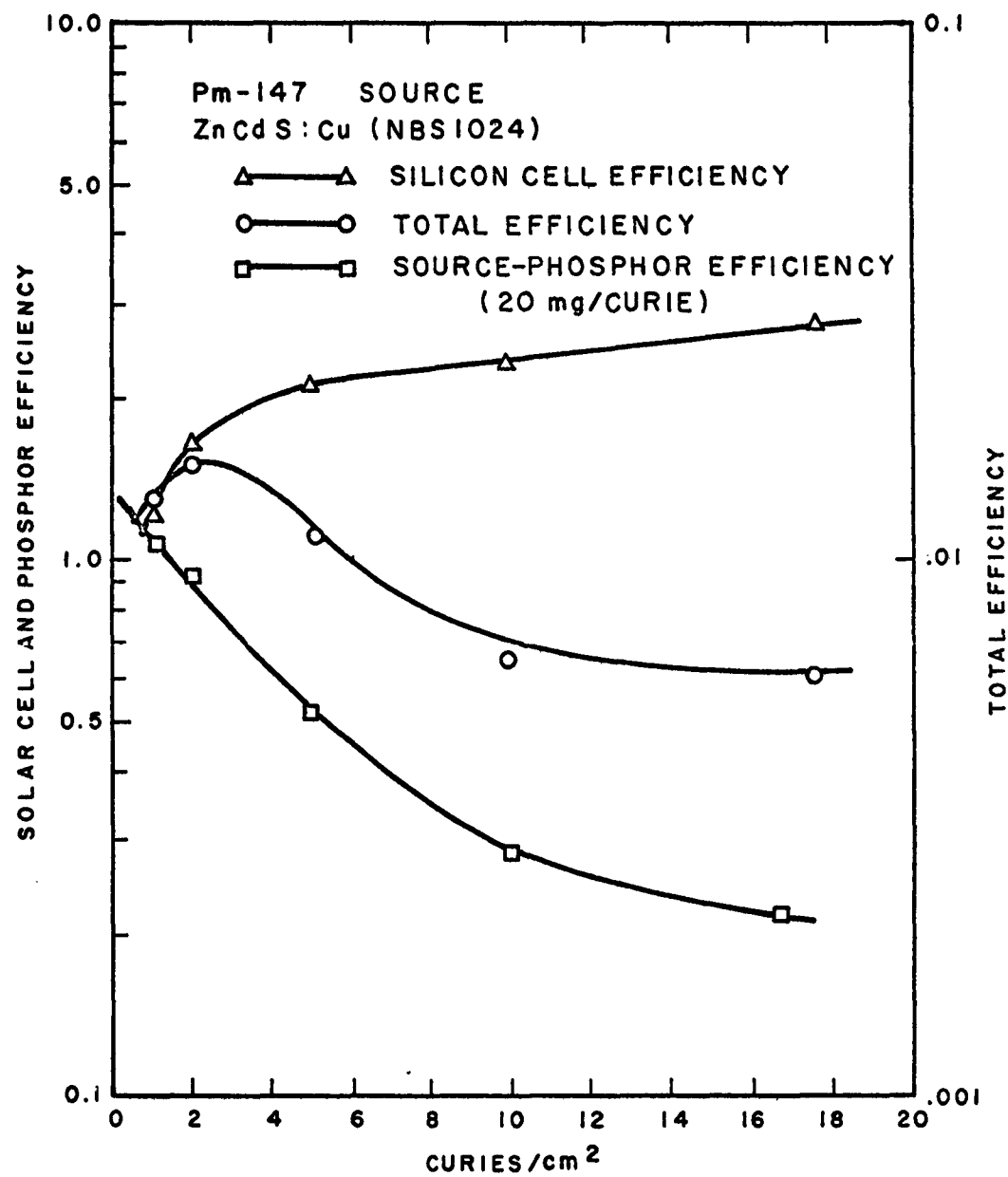


Figure 11

DEPENDENCE OF SOURCE-PHOSPHOR EFFICIENCY,
SILICON CELL EFFICIENCY, AND TOTAL EFFICIENCY
ON AMOUNT OF PROMETHIUM-147 PER UNIT AREA

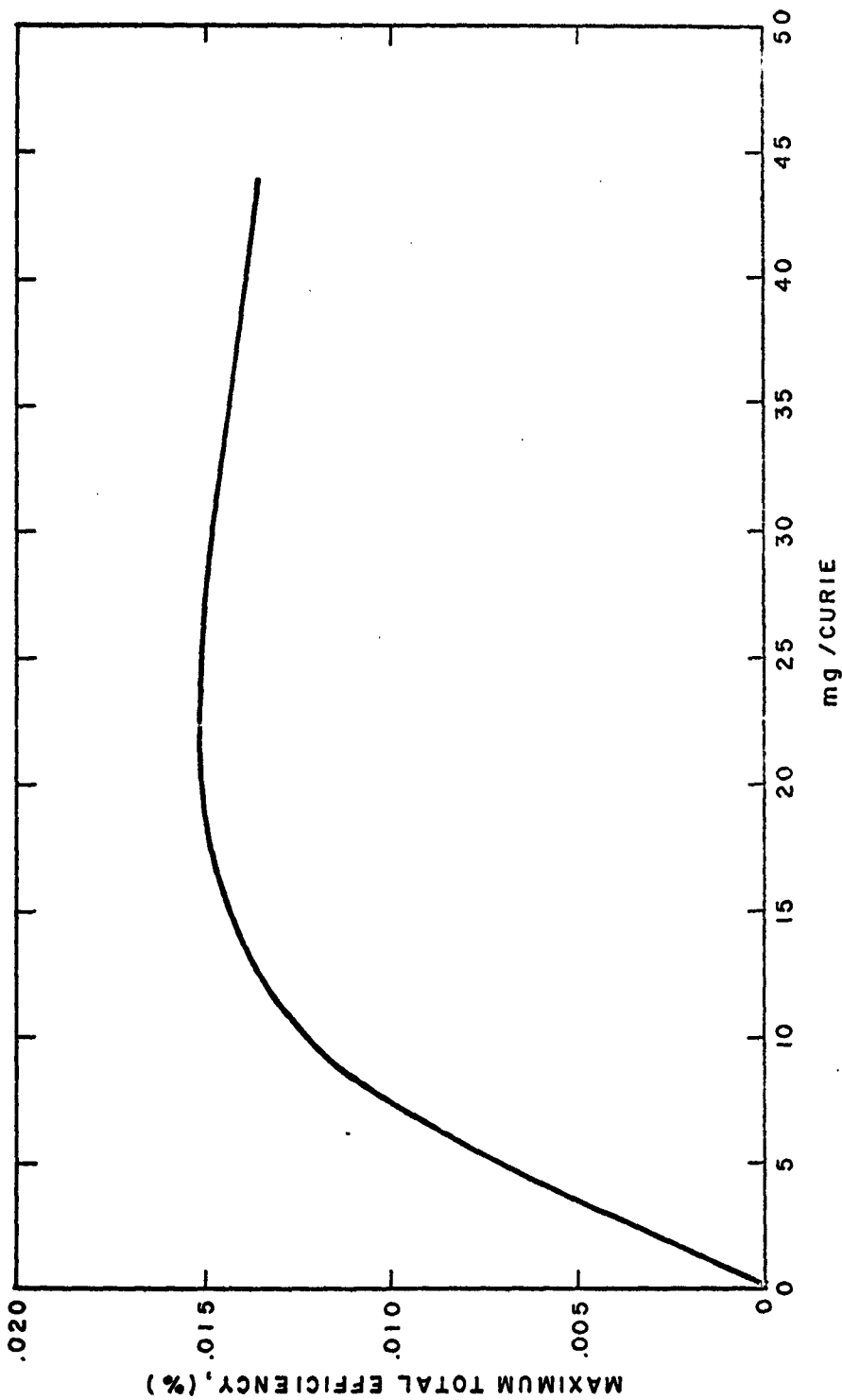


Figure 12
EFFECT OF PHOSPHOR-SOURCE RATIO (mg/curie) ON TOTAL EFFICIENCY

M_{pc} = mass of photovoltaic converter in mg/cm²

M_{sp} = mass of source-phosphor mix in mg/cm²

In the maximum efficiency case, $M_{pc} = 260$ and $M_{sp} = 20$ C; thus,

$$P/M = \frac{C\epsilon}{260 + 20 C}$$

Values of ϵ for a given C were taken from Figure 11, and the resultant curve of power per unit weight as a function of source loading is shown in Figure 13.

It is apparent in this case that a source loading of 4 to 5 curies/cm² would be the best choice for aerospace use where the weight and size of the power source is a significant factor. Also, it is apparent that an appreciable fraction of the total weight is consumed by the photovoltaic materials when using silicon. The use of a thinner or lighter photovoltaic converter would decrease the total weight and would bring the maximum power per weight loading nearer to the maximum efficiency loading.

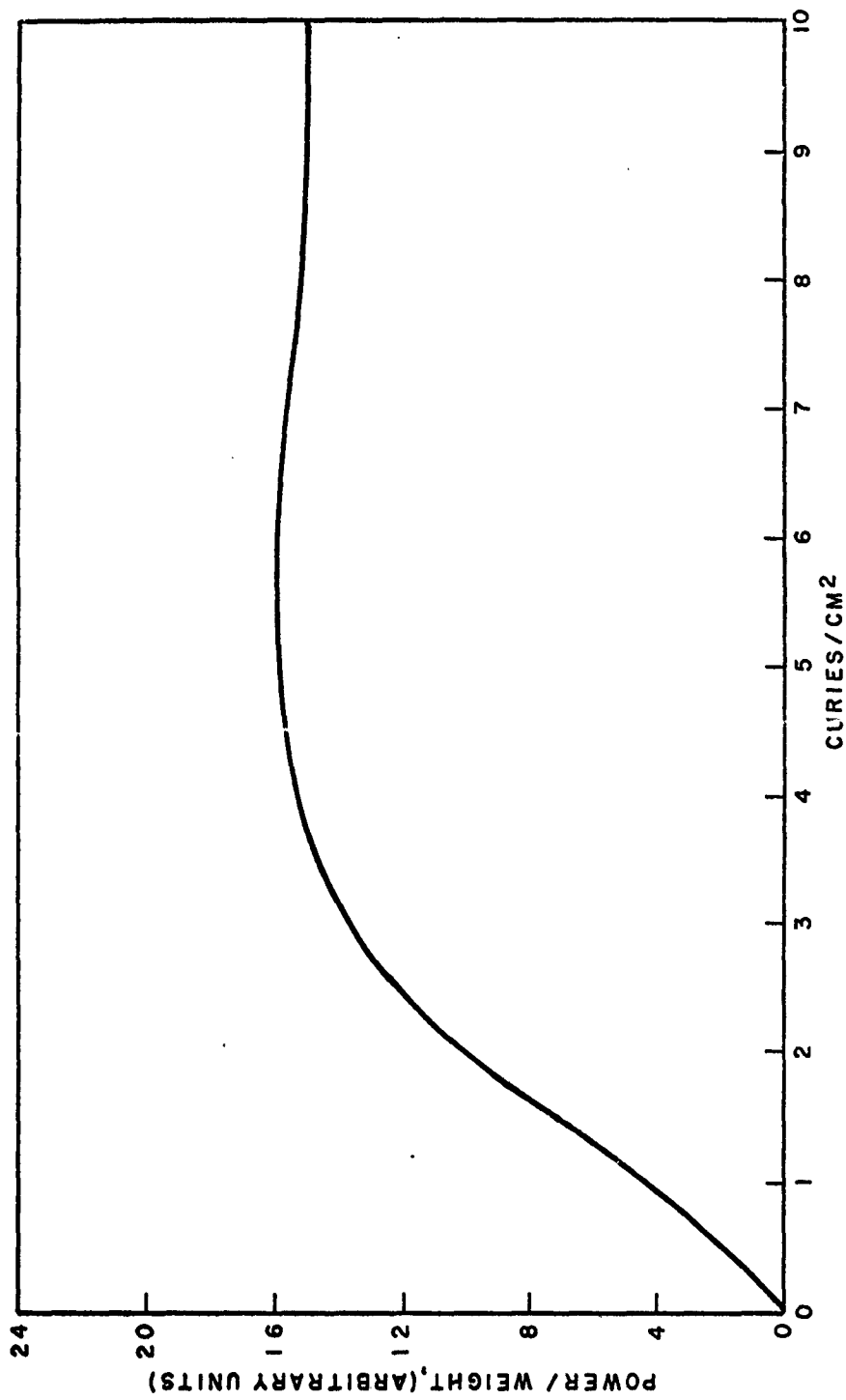


Figure 13
DEPENDENCE OF POWER PER UNIT WEIGHT ON AMOUNT OF
PROMETHIUM-147 PER UNIT AREA

PHOSPHOR-PHOTOVOLTAIC CONVERTER GEOMETRY

One problem in fully utilizing the luminescence from a phosphor is the internal light trapping and reflection losses at the boundary of a high refractive index material. This is especially true for large crystals of cadmium sulfide which has a refractive index of 2.5. For example, the critical angle for total internal reflection of a light ray in a material with a refractive index of 2.5 is $\sin \theta = 1/2.5$ when the boundary is air with an index of 1.0. This angle θ is 24° , i. e. only that light which strikes the boundary or surface at an angle less than 24° to the normal will leave the high index material. If the material's index were 1.5, this angle would increase to 42° . The reflection losses at normal incidence at a boundary of index 2.5 to index 1.0 would be $(2.5 - 1.0)^2/(2.5 + 1.0)^2 = 0.18$ or 18 percent. If the boundary were from index 2.5 to index 1.5, for example, the normal incidence reflection loss would drop to 6.2 percent. These numbers illustrating the importance of optical coupling apply strictly, only to clean flat surfaces. A powder phosphor mass is a diffuse optical material and the analysis of the light trapping and reflection losses is complex.

Bulk silicon has a refractive index of about 3.5 at 800 millimicrons. ("Anti-reflection" coatings are used on silicon solar cells to reduce the surface reflection losses.) An optimum optical coupling between a CdS phosphor and a silicon photovoltaic cell would be a transparent binder with a refractive index of about 3.0 in which both the phosphor surface and silicon surface are immersed. Unfortunately, there are no suitable optical coupling materials in this high index range. The common binders used in fluorescent screens and nuclear light sources have refractive indices of about 1.5. There is still an advantage in using binders even of this low index. In working with a prototype power cell consisting of a powdered ZnCdS: Cu phosphor in contact with a silicon cell, it was observed that the power output was increased by 13 percent when a parlodion in amyl acetate binder was used.

Single Crystal Phosphor - Photovoltaic Converter

A combined phosphor and photovoltaic converter in a single crystal would be the ultimate in optical coupling. A device of this type could be, for example, a large crystal of luminescent CdS with a rectifying barrier on the surface for the photovoltaic conversion. Besides the advantage of reduced optical coupling losses, this device could have a very low photovoltaic converter weight to source-phosphor weight ratio.

Cadmium sulfide photovoltaic cells have been fabricated and studied in both single crystal and evaporated thin film forms. Solar efficiencies of 3 percent have been reported (Ref. 28), and it is indicated that efficiencies twice that could be expected. Also, one could expect that CdS photovoltaic converters would be less sensitive to radiation damage and temperature than silicon cells. We do not know the characteristics of the CdS cell at low illumination intensities.

An important question in the consideration of a combined phosphor-photovoltaic converter is - can CdS material which is doped for luminescence be made into a good surface barrier cell without destroying the luminescence properties of the entire piece? Unfortunately, none of the large CdS crystals which were obtained were suitable luminescent materials. Assuming, however, that the dopant concentration for luminescent CdS may lie within the range of dopant concentrations available, preliminary experiments were performed with the aim of converting one surface of the CdS pieces into a photovoltaic barrier. The general scheme was to diffuse indium into one surface of the CdS to produce a nearly uniform, thin n-type layer to which a copper rectifying barrier was applied.

The starting materials for these experiments were large crystal pieces of CdS of four types: (1) "pure", i. e. not purposely doped, (2) lightly doped with copper (concentration unknown), (3) doped with 75 ppm copper, and (4) doped with 20 ppm silver and 40 ppm indium. The pieces were sectioned and lapped to thicknesses of about 3 millimeters. The pieces were placed in an evaporator and a layer of indium was deposited approximately 130 Angstroms thick on (1) and (2), and 11000 Angstroms thick on (3) and (4). After evaporation the samples were placed in a Pyrex tube which was evacuated, flushed with helium several times, then filled with helium to slightly under one atmosphere of pressure and sealed off. Diffusion was done in a furnace which had equilibrated at 610°C over a length longer than the sealed off Pyrex tube to insure that all portions of the tube were at a temperature at least equal to that of the CdS samples so that sublimation would be minimized. The tube was left in the furnace for 24 hours.

After the diffusion it was observed that all surfaces of the Ag, In doped sample (4) were covered with indium, probably indicating a saturation concentration. The indium was removed from the front surface of this sample and indium solder contacts were made to the sides of all four samples. Based on before and after resistance measurements on these samples, the indium did diffuse in and generate carriers. (It is known that indium is a donor for CdS). The sample surfaces on which the indium had been initially evaporated were roughened slightly and masked off around the edges; and the remainder of the crystal surfaces were masked off. Copper was then deposited electrochemically on the unmasked portion and the samples were post heated at 600°C for one minute, as prescribed in the literature (Ref. 29). Following this, a solder contact was made to the copper.

All four of the samples were found to be back-wall photovoltaic barrier cells, but with very low energy conversion efficiencies. At an illumination intensity of 2 mw/cm² of red light, sample (1) had a conversion efficiency of 10^{-4} percent; and at an illumination intensity of 10 mw/cm², sample (2) had an efficiency of 5×10^{-4} percent. The other two samples, (3) and (4), had much lower response, due to the increased optical absorption in the bulk CdS.

Time did not permit further experiments on these samples. The preliminary experiments performed do indicate that a photovoltaic barrier can be fabricated in heavily doped CdS. Further experiments on this combination device should probably await the starting material of large luminescent CdS crystals.

DESIGN OF TEN WATT POWER SOURCE

A conceptual design of a ten watt output power source has been made based on currently available materials. This design uses the source-phosphor powder mix geometry with Pm_2O_3 and ZnCdS: Cu sandwiched between two silicon junction photovoltaic converters. Before discussing the design, however, a description of experiments with a prototype unit power cell of this type is given next.

Prototype Unit Power Cell

A prototype unit power cell of the mixed source-phosphor type was constructed, using a silicon cell on only one side of the mix. A holder was constructed out of 4-inch diameter lucite with a hole drilled in the center to contain a one-inch diameter silicon photovoltaic cell. The cell was held at the bottom of the hole by a lucite retainer ring with a 15/16-inch inside diameter, and the leads were passed out through fine holes drilled in the lucite block. A 15/16-inch diameter polished lucite piston was threaded so that it could be screwed into the cylinder. The source-phosphor mix, containing 16.6 curies of Pm_2O_3 and 360 mg of NBS 1024 phosphor (ZnCdS: Cu), was poured on the top of the silicon and the piston was screwed down with only enough pressure to distribute the powder uniformly. Thus, over the 15/16-inch-diameter silicon (4.46 cm^2), the source concentration is 3.73 curies/ cm^2 and the loading ratio is 21.9 mg/curie.

The maximum power output, obtained at a load of 700 ohms, was measured as 1.47×10^{-6} watts, corresponding to 0.023 percent total efficiency. A solution of Parlodion in amyl acetate was then poured on top of the powder mix to determine whether a binder also has an optical coupling effect. It was observed that the Parlodion, whose refractive index is about 1.5, increased the power output by 13 percent to 1.66×10^{-6} watts at about a 35 mv photovoltage for the silicon cell used. The illumination intensity on the silicon cell was $22 \mu\text{w}/\text{cm}^2$, and the source-phosphor mix was, therefore, working at an efficiency of 1.55 percent per surface, or 3.1 percent total efficiency.

No significant change in power was observed whether the lucite plug was on top of the source-phosphor mix or was removed. Placing an aluminized reflector on top of the phosphor increased the power output by only 6 percent. This indicates that it is better to use a silicon cell on each side of the source-phosphor mix rather than using a reflector on one side.

Although the observed efficiency was only 0.026 percent, it is easily possible to raise this to better than 0.1 percent. Firstly, by placing a silicon cell on both sides of the phosphor the output and thus the efficiency is doubled, yielding an efficiency of 0.052 percent. Using the phosphor $(0.6)\text{Zn}(0.4)\text{CdS: Cu}$ in place of the NBS 1024 phosphor would (see Table 3) give another efficiency increase by a factor of 1.26, raising it to 0.0655 percent. The 1 cm x 2 cm "ten percent solar cell", whose efficiency versus illumination

intensity curve was shown in Figure 2, had an efficiency at these light intensities of twice that of the one-inch diameter cells used in this experiment. Thus by using a "ten percent" cell the efficiency would be 0.131 percent. Lastly, the source loading in this prototype was chosen for a better power per weight ratio rather than the best efficiency value. If the source loading were dropped to 2 curies/cm², the efficiency would be raised by the ratio 0.015/0.013 (see Figure 11), thus giving a maximum overall conversion efficiency of 0.151 percent.

The power output of this unit dropped by 20 percent during the first 100 hours of operation; then it stabilized and has remained constant for over 400 hours of operation. It was observed that the short circuit current drop during the first 100 hours was about 10 percent while the open circuit voltage dropped about 5 percent. This efficiency loss could be due to a decrease in source-phosphor output and/or some damage to the cell. Beta particle damage to the silicon cell could be overcome by laying down a thin layer of phosphor, about 20 mg/cm², on the silicon cells before depositing the source-phosphor mix.

Ten Watt Source Design

In designing a ten watt output power source based on currently available materials, we do make an optimistic assumption that the source will operate at 0.2 percent overall conversion efficiency. This is optimistic since the design will be using stacked unit power cells which will be operating at a temperature of about 100°C (see page 18), where the efficiency of the unit will be one-half of that at room temperature. Thus, we are assuming a room temperature efficiency of 0.4 percent, which is about three times the maximum efficiency mentioned for the prototype power cell. It is not unlikely that a better silicon photovoltaic cell could be obtained and that some improvements could be made in the source-phosphor mix by either using a slightly different ZnCdS: Cu phosphor or by a better mixing of the source and phosphor.

The design is for the best power per weight ratio, that is, a source loading of 4 curies/cm² and 20 mg/curie of phosphor. This power source would be a rectangular stack eight inches thick and five feet square. It would weigh 2500 pounds with a power per weight ratio of 4 mw/lb. Seventy six percent of the weight would be silicon cells, based on a figure of 130 mg/cm² for a silicon cell with contacts. A total of 1.3×10^7 curies of Pm-147 would be needed. The fabrication of the power source would be rather complex and very expensive. Further details of this power source, including a drawing of the conceptual design, are given in Appendix II.

Obviously, this power source would not be practical for aerospace use with such a low power per weight and efficiency. To be competitive with other power sources the power per weight ratio would have to increase by two to three orders of magnitude. Possible improvements in a double energy conversion source are discussed in the following paragraphs.

Future Improvements on Power Source

Starting with the power source described above, consider what factors of improvement may be made with the use of "ideal" materials. The power source based on currently available materials utilized a unit power cell weighing 345 mg/cm^2 , having an input phosphor excitation of 1.52 mw/cm^2 , a phosphor excitation density of about $19 \mu\text{w/mg}$, and operated at 0.2 percent efficiency at 100°C .

The first assumed ideal material is a large luminescent crystal of CdS with the same luminescent efficiency of the powdered phosphors used, and an optical half value thickness to its own luminescence emission of 1.0 cm. Use the source-phosphor geometry of source slots in a phosphor slab (Figure 9-B) with $h = 1.0 \text{ cm}$ and $S = P = 0.1 \text{ cm}$, the smallest practical spacings. In addition to what is shown in Figure 9-B, the phosphor slab should also have a top piece of thickness P so that photovoltaic converters can be placed on both the top and bottom phosphor surfaces. This source-phosphor geometry gives us 10 cm^2 of source surface per cm^2 of unit cell surface.

The ideal beta source for this geometry is Tl-204, thus the second assumption is that Tl-204 is available at its theoretical maximum specific activity. A "thick" source of thallium would have an excitation output of 5.47 mw/cm^2 of source surface and a phosphor excitation density of $39 \mu\text{w/mg}$ (see page 25). The total input phosphor excitation will then be 54.7 mw/cm^2 of unit cell, which is a gain of 36 per unit cell compared to the "currently available materials source". Assuming that 75 percent of the generated luminescence is lost by absorption in the CdS and the source slots, the gain of illumination intensity available in the phosphor at the top and bottom surfaces is reduced to 9.

Next, assume that the top and bottom surfaces of the CdS have been made into photovoltaic barriers whose efficiency characteristics are the same as a "ten percent silicon solar cell" (see Figure 2). Having the integral phosphor - photovoltaic converter in a single piece of CdS should reduce the light losses due to internal trapping and reflection (see page 39) by at least a factor of two. Thus the gain of illumination intensity on the photovoltaic converters should increase to 18. An increase of illumination intensity by a factor of 18 at these low intensities will increase the photovoltaic conversion efficiency by a factor of 10, so that the total gain in power per unit cell will be 180.

The weight of the "ideal" unit cell, however, will increase appreciably. Assume that the source material and phosphor have the same density ($\rho = 4.58 \text{ gm/cm}^3$), and that nearly all of the volume in the unit cell is filled. (For the lowest light losses an air interface between source and phosphor surfaces is desired.) Neglecting the weight of the contacts, the mass would then be equivalent to a 1.2 cm ($h + 2P$) thicknesses of CdS, or 5500 mg/cm^2 . This is a weight increase of a factor of 16 per unit cell. Thus, the power

per weight ratio of this "ideal" source would have increased by only a factor of 11.2.

Some of the factors used in the above illustration may be questionable, but it is believed that the power per weight gain calculated is correct within a factor of two to four. It should be noted that even though there was an appreciable increase in power per unit cell in the "ideal" case, the overall energy conversion efficiency would remain essentially identical to the design case. For example, in using "thick" beta sources only one-quarter of the total beta energy is used (see page 25), the slotted phosphor was assumed to have a light loss of one-quarter, the combined phosphor-photovoltaic converter increased the optical coupling by a factor of two, and the increased photovoltaic conversion efficiency was assumed to be a factor of ten. The relative total efficiency increase would then be $1/4 \times 1/4 \times 2 \times 10 = 20/16 = 1.25$. This "ideal" case is essentially a brute force method of increasing the illumination intensity on the photovoltaic converter.

The same power per weight increase could be obtained with the source-phosphor mix if a photovoltaic material which maintained its photovoltage or efficiency at low illumination intensities existed. If this were obtained, the overall conversion efficiency of the power source would also increase. Theoretically attainable efficiencies have been calculated for different materials as solar cells using p-n junction theory, but these calculations were made for high light intensities and they do not take into account, to a sufficient degree at least, effects at the junction itself. Calculations are made in Appendix III which cover (a) low light levels and (b) effects at the junction, to the extent of assuming a Shockley-Reed defect.

Since the short circuit current, i_s , is linear with the intensity of the absorbed radiation for any given wavelength, it follows that the desired condition is the same for either high or low light levels. That is, the condition is to collect as many radiation generated electron-hole pairs at the junction as possible. However, the problem of the photovoltage is different. As pointed out in the Appendix, the voltage at maximum power is proportional to the open circuit voltage, so that it is possible to discuss only the open circuit voltage as a good approximation. The open circuit voltage equation is

$$\ln \left[\frac{i_s}{i_o} + 1 \right] = \frac{eV_\infty}{akT},$$

hence, if i_s is small due to low light levels, it is imperative that i_o be as small as possible and a as large as possible. Now the crux of the problem lies in i_o , the reverse saturation current, since for large band gap materials this is strongly junction dependent. Further, it is true that a is junction dependent too, but it is a slowly varying quantity. It may be near to or even as high as three, as contrasted with the value of one for simple p-n junction theory. The importance of the state of the art of materials research is emphasized here since a large value of voltage for low light levels hinges upon it. Reference is again made to Appendix III for details.

CONCLUSIONS

1. If it were fabricated with currently available materials (Pm-147, ZnCdS:Cu powder, and silicon photovoltaic cells), a ten watt electrical output power source, based on a double energy conversion scheme with a beta emitting radioisotope as primary power, would have an overall energy conversion efficiency of about 0.2 percent and would weigh about 2500 pounds for a power per weight ratio of 4 mw/lb.
2. The power per weight ratio could probably be increased by a factor of ten to forty, with the same overall conversion efficiency, if the following set of "ideal" materials were available:
 - a) high purity thallium-204 of nearly theoretical maximum specific activity;
 - b) large transparent luminescent crystals of cadmium sulfide which have an optical half value thickness of 1.0 cm or greater; and
 - c) a cadmium sulfide photovoltaic surface barrier combined with the luminescent crystal.
3. The silicon photovoltaic converters are more adversely affected by increased temperature and nuclear radiation than the ZnCdS: Cu phosphors.
4. The rapid decrease in the silicon cell's photovoltage and conversion efficiency at low illumination intensities causes an appreciable loss in the efficiency of the power source. If a photovoltaic material with a conversion efficiency of better than ten percent at illumination intensities of $\mu\text{w}/\text{cm}^2$ were available, the total conversion efficiency and the power per weight ratio could be increased by an order of magnitude over that described in (1).
5. For aerospace use in the ten watt output range, this type of self powered double energy conversion source does not appear useable because of its low power per weight and the complexity of fabrication.

LIST OF REFERENCES

1. Silverman, J., Canadian Patent 621, 860; June 13, 1961.
2. "Miniature Atomic Battery Packs Five-Year Punch", Ind. Labs. 8, No. 4, 82-3 (1957).
3. Vavilov, V. S. et.al., "The Problem of Operation of 'Atomic' Current Sources with Double Energy Conversion," Soviet Phys. - Solid State 1, 748 (1959).
4. Dawson, L. H. "The Measurement and Evaluation of Luminous Materials", NRL Report 4655, Dec. 8, 1955.
5. Miller, C. G., et.al., "Radioisotope Use for Self-Luminous Highway Signs" U.S. Nuclear Corp., Quarterly Progress Report - June 1 - August 31, 1961, USNC 61-103.
6. Heller, A., Anbar, M., "Application of Radioisotopes in Luminous Devices, Part I - Survey of Self-Illuminating Systems," Israel Atomic Energy Commission, July 1962 (USAEC - 1 A - 730).
7. Senett, W. P. et.al., "Stability of Phosphors to Beta Radiation," Associated Nucleonics, Inc. June 24, 1960, NYO-9434.
8. Shepp, A., "Qualitative Conversion by Phosphors of the Energy of Beta Particles into Fluorescent Quanta," Technical Operations, Inc. Final Report, April, 1958, AD 154270.
9. Armour Research Foundation "Feasibility Study on New Nuclear Light Source," Final Report, Nov. 18, 1958, ARF Project A686, American Ass'n of Railroads.
10. Wilson, E. J., Hughes, J. D. H. "Atomic Light," Engineering, 497, April 17 (1959).
11. 3 M Company, Luminous Materials Section, Bulletin on 3 M Brand Self-Luminous Materials.
12. Hine, G. J., Brownell, G. L., Radiation Dosimetry Academic Press, Inc., New York (1956).
13. Evans, R. D., The Atomic Nucleus McGraw-Hill, New York (1955).
14. Nuclear Division, Martin Marietta Corp., Baltimore, Md., "⁹⁰Sr Fueled Thermoelectric Generator Power Source for Five-Watt U. S. Coast Guard Light Buoy," Final Report MND-P-2720 p. 29, (Feb. 2, 1962).

15. Kleinman, D. A., "Considerations on the Solar Battery," Bell Systems Tech. J. 40, 85 (1962).
16. Prince, M. B., and Wolf, M., "New Developments in Silicon Photovoltaic Devices," J. Bri. IRE 18, 583 (1958).
17. Pines, D., "Collective Energy Losses in Solids," Rev. Mod. Phys. 28, 184 (1956).
18. Garlick, G. F. J., "Excitation of Phosphors by Electrons," Brit. J. Appl. Phys. Suppl. No. 4, 103 (1954).
19. Gergely, Gy. "Notes on the Cathodoluminescence Efficiency of Zinc Sulfide Type Phosphors," J. Electronics and Control 5, 270 (1958).
20. Leverenz, H. N., An Introduction to Luminescence of Solids, John Wiley and Sons, Inc., New York (1950).
21. Bleil, C. N., et. al., "Bombardment of Cadmium Sulfide Crystals with 30- to 60-kev Electrons," Phys. Rev. 111, 1521 (1958).
22. Davoine, F., et. al., "Microscopic Observation of Cadmium Sulfide Bombarded with 5-kev Electrons," J. Phys. Rad. 21, 121 (1960).
23. Klick, C. C., "Luminescence and Photoconductivity in Cadmium Sulfide at the Absorption Edge," Phys. Rev. 89, 274 (1953).
24. Downing, R. G., "Electron Bombardment of Silicon Solar Cells," Vol. 3 Progress in Astronautics and Rocketry, Academic Press (1961).
25. Potter, A. E., "Solar Cells and Other Direct Conversion," Space Power NASA - University Conference, Session 14, November 3, 1962, Chicago, Illinois.
26. Pfann, W. G., van Roosbroeck, W., "Radioactive and Photoelectric p-n Junction Power Sources" J. Appl. Phys. 25, 1422 (1954).
27. Reiffel, L. and Kapany, N. S., "Some Considerations on Luminescent Fiber Chambers and Intensifier Screens", Rev. Sci. Instr. 31, 1356 (1960).
28. Shirland, R. A., et. al. "Large Area Thin Film Cadmium Sulfide Solar Cell", ASD TDR 62-69 (1962).
29. Rappaport, P., R.C.A. Review 20, 373 (1959).

APPENDIX I

DETERMINATION OF THE TEMPERATURE OF STACKED POWER UNITS

To develop an efficient power source using the principle of double energy conversion, space considerations require that individual radioisotope-phosphor-photovoltaic cell units be stacked in some manner. Since each of these units is a heat source as well as an electrical power source, there is a limit on the number of these units which may be present in a single stack while maintaining the maximum power output of each unit. This stack thickness limit is determined by consideration of the possible mechanisms of heat transfer from the stack and by the maximum temperature permitted for best efficiency (100°C).

The individual units consist of a slab of a mixture of powdered promethium oxide (Pm_2O_3) and powdered cadmium sulfide (CdS) sandwiched between two slabs of silicon (Si). The method of heat relief considered is radiation to black space from the ends of the composite.

Theoretical Considerations

For purposes of derivation, the composite of individual units can be assumed to be a uniform slab with constant thermal conductivity and uniform heat generation (Fig. 14).

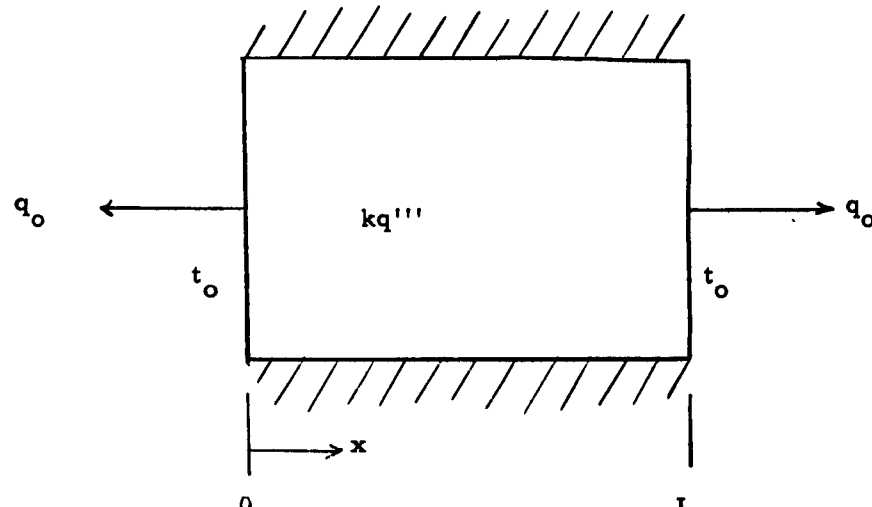


Fig. 14 - One-Dimensional, Steady Heat Flow Model

The temperature distribution within the composite (t) can be found as (Ref. 1):

$$t = t_o + \frac{q''' (L - x)x}{2k} \quad (1)$$

where k is the thermal conductivity, L is the composite thickness, q''' is the internal heat generation rate per unit volume, and t_o is the surface temperature of the end faces. The maximum temperature in the composite occurs at its center ($x = L/2$) and is given as:

$$t_m = t_o + \frac{q''' L^2}{8k} \quad (2)$$

The heat transfer rate at the ends (q_o) is given as:

$$q_o = \frac{q''' AL}{2} \quad (3)$$

where A is the constant cross sectional area.

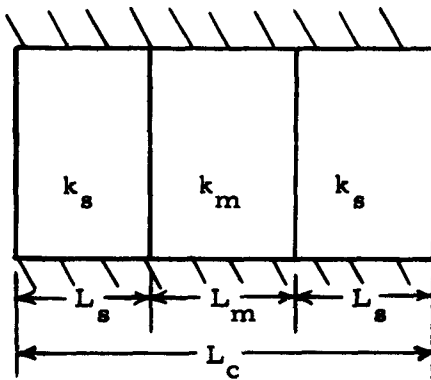


Fig. 15 - Individual Cell

In a stack of the individual power cells, the equivalent thermal conductivity is equal to the equivalent thermal conductivity of each cell. The thermal conductivity of a heterogeneous cell, shown in Figure 15, is given as:

$$k = \frac{L_c}{\frac{2L_s}{k_s} + \frac{L_m}{k_m}} \quad (4)$$

For radiation cooling to black space of the ends,

$$t_o = \left(\frac{q_o}{\sigma A \epsilon} \right)^{1/4} \quad (5)$$

Thus, substituting in (2) and (3),

$$t_m = \left(\frac{q''' 4}{2\sigma A\epsilon} \right)^{1/4} + \frac{q''' L^2}{8k} \quad (6)$$

where ϵ is the emissivity of the ends and σ is the Stefan-Boltzmann natural constant.

The assumption that the composite of individual cells can be represented by a uniform slab with uniform thermal conductivity and uniform internal heat generation is not completely true for small numbers of individual cells. The equivalent thermal conductivity of each cell no longer serves to represent the actual conductivity of each individual slab of the cell when only a few are stacked; for this situation a more rigorous analysis is necessary. The assumption of uniform internal heat generation may not be true for small stacks of individual cells.

Properties of Materials

The thermal conductivity and density of the materials under consideration were taken as the following:

Mixed powder of promethium oxide and cadmium sulfide;

$$\rho_m = 2.0 \text{ g/cm}^3 \text{ (assumed)}$$

$$k_m = 0.024 \text{ cal/cm sec K}^0 \text{ (assumed)}$$

Silicon; (Ref. 2)

$$\rho_s = 2.33 \text{ g/cm}^3$$

$$k_s = 0.258 \text{ cal/cm sec K}^0$$

Although the density and thermal conductivity of the mixture of powdered promethium oxide and powdered cadmium sulfide could not be obtained, an assumption was made. Since the mixture was considered to consist of about 90 percent cadmium sulfide and 10 percent promethium oxide, the density of the powder mixture was taken as approximately half that of the cadmium sulfide. This assumption may not be accurate, but it will not seriously effect the validity of the results since it was observed that the equivalent thermal conductivity had a secondary role in the determination of the maximum thickness.

Cell Specifications

Since the composition and heat generation rate of each cell are dependent upon the mass of each material per unit of cross-sectional area and the

heat generation rate per unit of cross-sectional area, respectively, the following values were assumed, based on experimental work:

$$M/A \text{ for the mixture} = 0.085 \text{ g/cm}^2$$

$$M/A \text{ for the silicon} = 0.130 \text{ g/cm}^2$$

and $q''' L_c = 0.00152 \text{ watt/cm}^2 (\sim 4 \text{ curies/cm}^2)$

$$L_s = 0.050 \text{ cm (with contacts)}$$

From these values and the preceding properties, the length of each slab, the cell length, and the equivalent thermal conductivity of the cells can be calculated. The results of these calculations are:

$$L_s = 0.050 \text{ cm}$$

$$L_m = 0.0425 \text{ cm}$$

$$L_c = 0.1425 \text{ cm}$$

$$k = 0.066 \text{ cal/cm sec K}^0$$

$$q''' = 2.545 \times 10^{-3} \text{ cal/cm}^3 \text{ sec}$$

Allowable Composite Thickness

Combination of the above cell specifications with the relationships for the composite temperatures yields the maximum tolerable thickness of the stack of individual cells for a maximum allowable internal temperature of 100°C. For radiant cooling to black space of the ends, the assumption was made that, the emissivity is unity ($\epsilon = 1$). The Stefan-Boltzmann constant, σ , was used as $1.372 \times 10^{-12} \text{ cal/cm}^2 \text{ sec K}^4$. Then, from equation (6) the maximum tolerable thickness of the composite of individual cells (L) was found to be 20.1 cm. This thickness corresponds to a stack of approximately 140 individual cells. For this mode of heat transfer, it is readily seen from the above equation for the maximum length that the thermal conductivity of the materials plays a secondary role in the determination of the maximum thickness. The radiation rate almost entirely determines the maximum allowable thickness.

The results of the above calculations show that in order to increase the total input to a system employing the previously described power cells it is necessary to increase the total volume of material by increasing the cross-sectional area of a composite of cells whose thickness is below the calculated maximum. For a total input of 990 watts in the form of heat (corresponding to a 1 percent efficient 10 watt power source) the necessary cross-sectional area is given as:

$$A = 4630 \text{ cm}^2$$

It should be noted at this point that if the physical environment of the composite is such that radiant heat transfer is allowable only at one end of the composite, then the maximum allowable thickness must be halved and the cross-sectional area must be doubled to maintain the same input.

Discussion

The assumption that the composite of individual cells can be represented by a slab with uniform thermal conductivity and uniform internal heat generation is valid, considering the above results, since a large number of individual cells comprise the composite. Although the heat generation within any one cell may not be uniform, the heat generation within the composite may be taken as uniform since there are many such cells.

The assumption that heat relief of the power generation system is by radiation from the ends of the composite to black space was made since the system will be housed in a vehicle in space. The optimum heat relief scheme for a system of this type is one in which the heat relief is accomplished by the system itself. Since ultimately all the heat generated within the composite must be radiated away from the vehicle, any heat relief scheme other than that assumed for this analysis would only tend to either consume some of the power generated or greatly increase the systems dimensions, due to the fact that radiation of the same amount of heat at a lower temperature requires a considerably greater area.

To accomplish the assumed heat relief scheme in practice, the entire composite may, if possible, be mounted on the vehicle in the form of a fin, in which case the radiation will be from both ends as well as the sides of the composite. The radiation from the sides of the slab, which was not considered in this simplified analysis, will aid in the heat relief problem. If it is impractical to mount the system as a fin, it may be mounted in such a fashion that one end of the composite forms the surface of the vehicle. In this case, radiation is from only one end of the composite which is a less desirable condition.

The composite can be coated with a thin layer of electrical insulating material and contained by a metal skin in contact with the composite. The skin can be painted with any suitable high emissivity substance.

The maximum permissible thickness of the composite of individual cells could be increased greatly if the temperature limitations of the materials could be raised.

References

1. Jakob, M. and Hawkins, G. A., Elements of Heat Transfer, J. Wiley and Sons, New York, 1957.
2. Goldsmith, A., Watermann, T. and Hirschhorn, H., Handbook of Thermo-Physical Properties of Solid Materials, MacMillan, New York, 1961, Vol. I and III.

APPENDIX II

CONCEPTUAL DESIGN OF TEN WATT POWER SOURCE BASED ON CURRENTLY AVAILABLE MATERIALS

The basic materials needed are:

- 1) 1.3×10^7 curies of Pm-147 in the chemical form of high purity (>90%) processed Pm_2O_3 ;
- 2) 580 pounds of (0.6)Zn(0.4)CdS: Cu powdered phosphor;
- 3) $6.55 \times 10^6 \text{ cm}^2$ of high efficiency silicon junction photovoltaic cells (each cell should be square or rectangular and of as large an area as possible); and
- 4) about 10 pounds of a transparent high refractive index phosphor binder (the choice of binder could best be made with proprietary information from commercial suppliers of high brightness nuclear light sources).

The source (1) and phosphor (2) are mixed together in the ratio of 20 milligrams of phosphor to one curie of source.

A unit power cell consists of a sandwich of source-phosphor mix, at a source concentration of 4 curies/cm², between two silicon photovoltaic cells (3). A minimum amount of binder (4) should be used in the mix, and the sandwich should be put together before the binder has set so that both the silicon cell surface and the phosphor are immersed in the same optical medium.

The unit cells are then put into a flat, close packed array of $2.34 \times 10^4 \text{ cm}^2$ (about 5 feet x 5 feet). The adjacent silicon cells, i. e. all of the top silicon cells and all of the bottom silicon cells, are connected in parallel. One hundred and forty of these large area arrays must be made.

The layer arrays of unit cells are stacked, surface to surface, as shown in Figure 16. The layers of silicon cells which back up to one another are electrically connected in parallel. Likewise, the two outermost layers of silicon cells are paralleled, so that the entire stack consists of 140 individual and identical parallel power sources. These 140 source are then connected in series. Assuming that each silicon cell has a photovoltage of about 75 millivolts at maximum power load, the output voltage would be 10.5 volts at 10 watts.

The entire composite can be coated with a thin layer of electrical insulating material and contained by a metal skin in contact with the large area surfaces. The outer metal skin should be made to have a high emissivity (by painting or coating a suitable material on it).

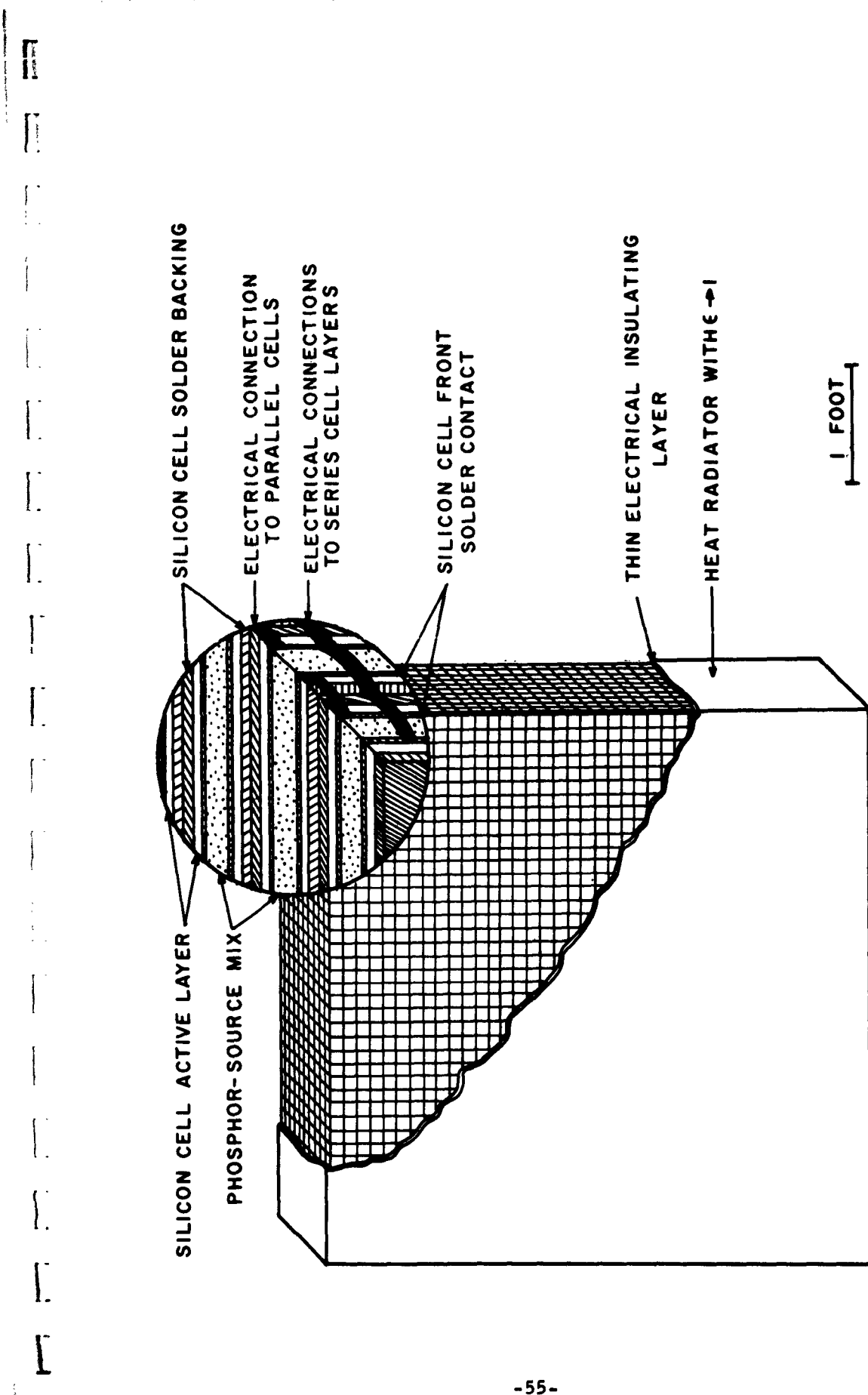


Figure 16
CONCEPTUAL DESIGN OF TEN WATT POWER SOURCE

The outer dimensions of the source are 8 inches x 5 feet x 5 feet. It would weigh about 2500 pounds, of which 76 percent by weight is silicon. The power source is designed to operate at an internal temperature of 100°C when its heat loss is by radiation to black space.

The output of this power source should essentially follow the half life of Pm-147, i. e. after 2.6 years the output will be one-half of the original power.

APPENDIX III

PHOTOVOLTAIC EFFICIENCY AND LARGE BAND GAP SEMICONDUCTORS

The reduced efficiency of silicon photovoltaic cells at low light levels, such as are obtained from phosphors, is a major factor in the overall low efficiencies observed in this study of nuclear-photon energy converters. In this Appendix this problem is discussed from the standpoint of p-n junction theory and it is shown that a solution lies in the advancement of the state of the art of the larger band gap semiconductors for which a p-n junction approach is applicable. The problem is first discussed generally and following this a specific material, cadmium telluride (CdTe), is considered as an example for calculations.

Open Circuit Photovoltage and the Reverse "Saturation" Current

The equation for the open circuit photovoltage can be obtained from the photocurrent equation,

$$i = i_s - i_o e^{-eV/akT},$$

by letting the photocurrent go to zero. Since the photocurrent, i , is non-negative it follows that for a given short circuit current, i_s , one gets the largest value of photovoltage, V , for the condition, $i = 0$. This maximum value, V_∞ , is related to the voltage at maximum power transfer by the equation

$$e^{eV_{mp}/akT} (1 + e^{eV_{mp}/akT}) = e^{-eV_\infty/akT}.$$

and since the voltage at maximum power transfer, V_{mp} , is a monotonically increasing function of V_∞ , one can treat the problem from the simpler viewpoint of the open circuit voltage. Letting the photocurrent, i , go to zero in the above equation, one obtains the desired relation between V_∞ and the short circuit current, i_s , and the reverse "saturation" current, i_o

$$\ln \left(\frac{i_s}{i_o} + 1 \right) = eV_\infty/akT.$$

Now this equation has turned out to be experimentally verifiable to a good approximation, and will serve as the basis for a discussion of efficiency at low light levels compared to high light levels.

Experimentally, it has been found that for a given cell the short circuit current is proportional to the light intensity. Based, therefore, upon short circuit current considerations only, the efficiency should not change from high light levels to low. The fact that it does change indicates that the problem is not with the current but with the voltage of the cell. For further discussion, let us consider i_s is a constant; the factors then at room temperature which determine the voltage are i_o and a . Now a would be equal to unity if the simple, diffusion theory were applicable to the p-n junction, but experimentally it is found to be around two for silicon cells. This suggests that the simple theory of the p-n junction, in which the junction itself is neglected, is not applicable to silicon. This point has been made within recent years, and the importance of effects at the junction have been stressed.

Before getting more deeply involved with the junction itself, let us consider the following data taken from a paper by J. J. Loferski (Ref. 1) (only part of the table is being reproduced);

<u>Material</u>	<u>Bandgap (eV)</u>	<u>Lifetime (Minority Carrier)</u>	<u>N_D (cm⁻³)</u>	<u>i_o (amp/cm²)</u>
Si	1.12	10^{-5} sec.	10^{17}	5.9×10^{-12}
InP	1.25	10^{-8}	10^{17}	1.9×10^{-14}
GaAs	1.35	10^{-8}	10^{17}	4.1×10^{-16}
CdTe	1.45	10^{-8}	10^{17}	1.2×10^{-19}

The meaning of the various terms will be discussed, but the important point to be stressed is that the calculations are based upon the simple, diffusion theory of the p-n junction.

A specific calculation will be made for cadmium telluride (CdTe) in the next section, and the meaning of most of the terms of the table will be made clear. N_D , however, is not used later; this refers to the density of donors and since the donors in these materials have ionization energies in the 0.04 electron volt or less level, it is a good approximation to consider N_D as equal to the number of majority carriers at room temperature.

The main point of emphasis at this time is on the values of i_o , the reverse "saturation" current (italics are used because saturation does not occur for silicon and such band gap materials). This again is due to a junction effect, principally. Consider, for calculational purposes, a short circuit current, i_s , of one microampere per cm² on a CdTe cell for which the i_o value is applicable. Recall that for a good silicon solar cell under bright sun conditions, the short circuit current is more than 10 milliamperes, so that the one microampere being considered would - for a good cell - be classed as a low light level. Putting these values in the open circuit voltage equation, letting $a = 1$, and neglecting the unity on the lefthand side one has

$$\ln (10^{-6}/1.2 \times 10^{-19}) = eV_{\infty}/kT = eV_{\infty}/0.026$$

$$\text{or } V_{\infty} = 0.77 \text{ volts open circuit.}$$

Note that in a silicon cell, the V_{∞} under comparable current is 0.05 volt or less usually. Returning again to the CdTe cell, if simple pn junction theory were applicable, and if leakage currents could be reduced to values less than i_0 , one would have a very useful photovoltaic material. Today, the bandgap of CdTe is considered to be 1.5 eV, not 1.45 eV, and hence the voltage would even be larger. However, just as in silicon, the junction itself cannot be neglected; in fact, it is more essential to consider it in CdTe.

Calculations for CdTe

The idealized model of the pn junction based upon diffusion theory neglects generation and recombination effects in the space charge region and as an approximation it appears valid only in the presence of appreciable diffusion currents in the forward and reverse direction such as for germanium at room temperature. In fact, one might expect it to work generally only for low band gap materials with appreciable minority carriers. For silicon, the reverse current does not saturate as expected from the idealized model and it may also be two to four orders of magnitude larger than the calculations indicated by diffusion theory. If one considers that the alpha, α , value in the photovoltage equation is around two, one can interpret it as a function of the injection level in the junction itself as due to generation and recombination due to localized recombination centers in the space charge region.

Since CdTe has a band gap of 1.5 eV, generation and recombination in the space charge region might be expected to be even more important than in silicon. To estimate the actual importance of space charge a calculation is made based upon the ideal theory using the current effective mass values for electrons and holes; and following this a calculation is made for CdTe based upon a Shockley-Reed mechanism following Sah, et. al. (Ref. 2) who found this to be a fairly good approximation for silicon.

Assume a 3 ohm-cm material, and for simplicity let us consider only the contribution due to the electrons as minority carriers on the p-side of the junction. From the np product approximation,

$$\begin{aligned} np &= N_c N_v e^{-Eg/kT} \\ &= 3.8 \times 10^{36} e^{-1.5/0.026} \text{ (room temperature),} \end{aligned}$$

using $0.1 m_0$ as the effective mass for electrons, and $0.3 m_0$ as the effective mass for the holes. Then with the band gap of 1.5 eV one has that

$$np = 3 \times 10^{11} \text{ cm}^{-6}.$$

Now, for a 3 ohm-cm material, p-type, one has

$$p = 2 \times 10^{16} \text{ (mobility holes, } 100 \text{ cm}^2/\text{volt sec})$$

and hence

$$n = 1.5 \times 10^{-5}.$$

For the number of electrons which diffuse over the junction per second, one considers the thermal generation rate, G , and assumes the random motion of the electrons averages out to the approximation that all carriers generated within a diffusion length, L , of the junction will go over. Therefore, the current due to the electrons per cm^2 is

$$i_{oe} = eGL.$$

To check this dimensionally, G is a number per sec per cm^3 $\times L$ in cm and this multiplied by charge leads to a current per cm^2 . Now since under equilibrium conditions the recombination rate, R , is equal to G and for a constant minority lifetime, $R = n/\tau$, then

$$\begin{aligned} i_{oe} &= e \frac{n}{\tau} L = e \frac{n}{\tau} (D\tau)^{1/2} \\ &= e n (D/\tau)^{1/2}. \end{aligned}$$

Assuming further that τ , is 10^{-8} seconds - as used before - and using for the diffusion constant, D , a value of $18 \text{ cm}^2/\text{sec}$ at room temperature, then

$$\begin{aligned} i_{oe} &= 1.6 \times 10^{-19} \times 1.5 \times 10^{-5} \times (18 \times 10^8)^{1/2} \\ &= 1.1 \times 10^{-19} \text{ amperes per cm}^2. \end{aligned}$$

Note, this is close to the value given before which was calculated for slightly different conditions. For a comparable lifetime, the value of i_{oh} for the holes would add about 30 percent. To get a feeling for this number, consider it means that less than one electron per second per cm^2 contributes to the current.

With such extremely small diffusion currents, even for minority carrier lifetimes in the 10^{-8} second region, it is quite certain that the generation and migration of carriers in the space charge region of the junction will dominate the diffusion current even for a nearly perfect junction.

Now, assume the existence of recombination centers near the middle of the band gap - Shockley-Reed model - let us calculate, following Sah, et. al., an approximate value for i_0 with a symmetric junction having the parameters listed previously: 3 ohm-cm material and a minority carrier lifetime of 10^{-8} seconds. Further, for simplicity, assume an abrupt junction. Roughly then, one gets a junction width of about 2000 angstroms. The generation rate in the junction with this model is

$$G_j = \frac{n_i}{2\tau}$$

where n_i is the intrinsic concentration of electrons - the square root of the np product, $3 \times 10^{11} \text{ cm}^{-3}$ - approximately $5.5 \times 10^5 \text{ cm}^{-3}$ at room temperature. τ , is taken as 10^{-8} seconds. Combining this with a junction width W of 2000 angstroms, one has

$$\begin{aligned} i_o (\text{junction}) &= \frac{en_i}{2\tau} \times W \\ &= \frac{e \times 5.5 \times 10^5 \times 2 \times 10^{-5}}{2 \times 10^{-8}} \\ &= 8.8 \times 10^{-11} \text{ amperes per cm}^2 \end{aligned}$$

Physically, the idea is that the carriers generated in the junction will not recombine in the junction but will be swept in the strong electric field to one side or the other depending upon the sign of the carrier. This is reasonable since for the hole which has a much smaller mobility than the electron, the transit time across 2000 angstroms is less than 10^{-11} seconds. Therefore, with a minority carrier lifetime of 10^{-8} seconds, there is a very small probability of recombination in the junction itself.

By comparing the reverse current under these two conditions one sees that generation and recombination current is almost 10^9 or nine orders of magnitude greater than the diffusion current. However, this is not as bad as it appears if one considers that the alpha, α , value in the photovoltaic equation is now two.

Putting these new values into the open circuit photovoltage equation in which i_s is one microampere, and again neglecting the unity, one has

$$\ln (10^{-6} / 8.8 \times 10^{-11}) = eV_\infty / 2kT = eV_\infty / 0.052$$

or $V_\infty = 0.48 \text{ volts.}$

If the minority carrier lifetime could be reduced to 10^{-7} seconds, and the leakage current restricted to values less than i_o , one would obtain an open circuit voltage of 0.59 volts with a one microampere short circuit current. It follows therefore that the possible direction to look for higher efficiency nuclear photon energy converters for which the light level is low is toward the larger band gap materials. However, the state of the art must be advanced for these semiconductors; probably, the closest approach to date would be in a GaAs cell.

References

1. Lofersky, J. J., J. Appl. Phys. 27, 777, (1956).
2. Sah, C., Noyce, R., Shockley, W., Proc. IRE 45, 1228, (1957).

Aeronautical Systems Division, Dir/Aero-
nautics, Flight Accessories Lab.,

Wright-Patterson AFB, Ohio.
Ref. No. AF-TRD-65-264. A NUCLEAR-PHOTON ENERGY
CONVERSION STUDY. Final Report, Mar 65, 61 pp. Incl.
111xx, tables, 35 refs.

Unclassified Report

1. Nuclear-photon energy converter
2. Radiotiscope beta source
3. Photovoltaic converters
4. Photophore

1. AFDC Project 6175, Task 617501-17
2. Contract No. AF 38 (657)-3627

3. Armour Research Foundation or III. Institute of Technology, Chicago, Illinois.
4. H. V. Wartke, R. D. Oestreich, R. J. Robinson

(over)

(over)

V. Avail fr ORS

VI. In AFIA collection

V. Avail fr ORS
VI. In AFIA collection

V. Avail fr ORS
VI. In AFIA collection

(over)

(over)

Aeronautical Systems Division, Dir/Aero-
nautics, Flight Accessories Lab.,
Wright-Patterson AFB, Ohio.
Ref. No. AF-TRD-65-264. A NUCLEAR-PHOTON ENERGY
CONVERSION STUDY. Final Report, Mar 65, 61 pp. Incl.
111xx, tables, 35 refs.

Unclassified Report

A double energy conversion technique was studied for
aeroplane use as a radiotiscope powered 10 watt electrical
output power source. In this technique, beta particles
from a radiotiscope are absorbed by a luminescent material
which emits a multiplicity of low energy photons.
These photons are then converted to electrical energy by a
photovoltaic device. The three components (radiotiscope,
photopher, and photovoltaic cell) are discussed individually
and then in combination in various geometries of source-

1. Nuclear-photon energy conversion
2. Radiotiscope beta source
3. Photovoltaic converters
4. Photophore

1. AFDC Project 6175, Task 617501-17
2. Contract No. AF 38 (657)-3627

3. Armour Research Foundation or III. Institute of Technology, Chicago, Illinois.
4. H. V. Wartke, R. D. Oestreich, R. J. Robinson

(over)

(over)

photopher and photophore-photovoltaic converter. Nuclear
radiation effects on the photopher and photovoltaic materials
restrict the choice of the radiotiscope to a low
energy beta emitter; and temperature effects limit the
number of "hot" power cells which may be attached in one
module. These effects are more pronounced in silicon
photovoltaic converters than in SiO₂: Cu type photophore.
A ten watt output power source fabricated with currently
available materials (Pb-147, silicon Cu, and silicon photov-
oltaic cells) would have an overall energy conversion
efficiency of about 0.8 percent and a power per weight
ratio of 4 mW/g. It is estimated that the power per
weight could be increased by a factor of ten to forty if
certain "ideal" materials were available. The rapid
decrease in photovoltage and energy conversion efficiency
of silicon cells at low illumination intensities causes
an appreciable loss in the overall efficiency of such
power source.

photopher and photophore-photovoltaic converter. Nuclear
radiation effects on the photopher and photovoltaic materials
restrict the choice of the radiotiscope to a low
energy beta emitter; and temperature effects limit the
number of "hot" power cells which may be attached in one
module. These effects are more pronounced in silicon
photovoltaic converters than in SiO₂: Cu type photophore.
A ten watt output power source fabricated with currently
available materials (Pb-147, silicon Cu, and silicon photov-
oltaic cells) would have an overall energy conversion
efficiency of about 0.8 percent and a power per weight
ratio of 4 mW/g. It is estimated that the power per
weight could be increased by a factor of ten to forty if
certain "ideal" materials were available. The rapid
decrease in photovoltage and energy conversion efficiency
of silicon cells at low illumination intensities causes
an appreciable loss in the overall efficiency of such
power source.